Entanglement certification from theory to experiment

*Nicolai Friis[1], Giuseppe Vitagliano[1], Mehul Malik[1,2] and Marcus Huber[1]**

Abstract | Entanglement is an important resource for quantum technologies. There are many ways quantum systems can be entangled, ranging from the two-qubit case to entanglement in high dimensions or between many parties. Consequently, many entanglement quantifiers and classifiers exist, corresponding to different operational paradigms and mathematical techniques. However, for most quantum systems, exactly quantifying the amount of entanglement is extremely demanding, if at all possible. Furthermore, it is difficult to experimentally control and measure complex quantum states. Therefore, there are various approaches to experimentally detect and certify entanglement when exact quantification is not an option. The applicability and performance of these methods strongly depend on the assumptions regarding the involved quantum states and measurements, in short, on the available prior information about the quantum system. In this Review, we discuss the most commonly used quantifiers of entanglement and survey the state-of-the-art detection and certification methods, including their respective underlying assumptions, from both a theoretical and an experimental point of view.

Quantum entanglement rose to prominence as the central feature of the famous thought experiment by Einstein, Podolsky and Rosen[1]. Initially disregarded as a mathematical artefact showcasing the supposed incompleteness of quantum theory, the properties of entanglement were largely ignored until 1964, when John Bell proposed an experimentally testable inequality able to distinguish between the predictions of quantum mechanics and those of any local-realistic theory[2]. With the advent of the first experimental tests emerged the realization that entanglement constitutes a resource for information processing and communication tasks, confirmed in a series of experiments[3–6]. With the development of quantum information theory, the understanding of entanglement has advanced and diversified, and many links have been established with other disciplines. Today, the study of Bell-like inequalities[7] is an active field of research, and recent experimental tests closed all loopholes[8–10], proving that entanglement is an indispensable ingredient for the description of nature and that quantum technologies can produce, manipulate and certify it.

However, in the early days of quantum information, Werner had already realized that entanglement and the violation of Bell inequalities are not necessarily the same phenomenon[11]. Whereas entanglement is needed to violate Bell inequalities, it is still not known whether (and in what sense) entanglement always allows for Bell violation[12–15]. From a contemporary perspective, Bell inequalities are seen as device-independent certifications of entanglement. However, the question of whether all entangled states can be certified device-independently is still an open problem. In the same paper, Werner also gave the first formal mathematical definition of entanglement. Since then, entanglement theory as a means to characterize and quantify entanglement has developed into an entire sub-field of quantum information. Previous reviews have captured various aspects of the research in this sub-field, focusing, for example, on the nature of non-entangled states[16] and on the quantification of entanglement as a resource[17,18], or providing detailed collections of works on entanglement theory[19] and entanglement detection[20].

In quantum communication, certifiable entanglement forms the basis for the next generation of secure quantum devices[21–24]. However, it is important to note that entanglement certification goes beyond entanglement estimation, in the sense that the latter may rely on reasonable assumptions about the system state or measurement setup, whereas the requirements for certification are stricter. In quantum computation, the certified presence of entanglement points towards the use of genuine quantum resources, which is crucial for trusting the correct functionality of devices[25]. In a quantum simulation, a large amount of entanglement can serve as an indicator of the difficulty of classically simulating the corresponding quantum states[26–28]. Nonetheless, the precise role of entanglement in quantum computation and simulation is less clear-cut than in quantum communication. Finally, entanglement can be understood as a means of bringing about speed-ups[29–31], parallelization[32]

[1]*Institute for Quantum Optics and Quantum Information (IQOQI), Austrian Academy of Sciences, Vienna, Austria.*

[2]*Institute of Photonics and Quantum Sciences (IPaQS), Heriot-Watt University, Edinburgh, UK.*

**e-mail: marcus.huber@univie.ac.at*

https://doi.org/10.1038/s42254-018-0003-5

Key points

- Entanglement detection and certification are of high significance for ensuring the security of quantum communication, improving the sensitivity of sensing devices, and benchmarking devices for quantum computation and simulation.
- Recent years have seen continuous progress in the development of tools for entanglement certification and an increase in control over a wide variety of experimental setups suitable for entanglement creation.
- Goals for the development of entanglement detection techniques are device-independence and assumption-free certification.
- Current challenges include the extension of well-understood methods for two qubits to many-body and/or high-dimensional quantum systems and their application in entanglement experiments with ions, atoms and photons.
- An important focus of recent research is the reduction in the number of measurements required for entanglement certification to cope with increasing system dimensions.

and even flexibility[33] in quantum metrology[34]. It is not a coincidence that these four areas also form the central pillars of the European flagship programme on quantum technologies[35].

With the development of the first large-scale quantum devices and more complex quantum technologies come the challenges of experimentally certifying and quantifying entanglement in quantum systems too complex for conventional tomography. These problems arise in finite-dimensional systems, which are the focus of this Review; for continuous-variable entanglement and infinite-dimensional systems, we refer the interested reader to existing reviews[36–38].

Entanglement detection and quantification

Entanglement and separability

Entanglement is conventionally defined through a contrapositive: separability. A pure quantum state is called separable with respect to a tensor factorization $\mathcal{H}_A \otimes \mathcal{H}_B$ of its (finite-dimensional) Hilbert space if and only if it can be written as a product state $|\psi\rangle_{AB} := |\phi\rangle_A \otimes |\chi\rangle_B$. A general (mixed) quantum state ρ is called separable if it can be written as a probabilistic mixture of separable pure states[11].

$$\rho_{\text{sep}} := \sum_i p_i \left|\phi_i\right\rangle\!\left\langle\phi_i\right|_A \otimes \left|\chi_i\right\rangle\!\left\langle\chi_i\right|_B \qquad (1)$$

All the infinitely many pure state decompositions of a density matrix can be interpreted as a concrete instruction for preparing the quantum state via mixing the states $|\phi_i\rangle_A |\chi_i\rangle_B$ drawn from a classical probability distribution $\{p_i\}_i$. Because each of these pure states is separable, mixed separable states can easily be prepared by coordinated local operations, that is, local operations and classical communication (LOCC)[39,40]. Conversely, any state that is not separable is called entangled and cannot be created by LOCC. The fact that there are infinitely many ways to decompose a density matrix into pure states is at the root of the central challenge in entanglement theory: to conclude that a state is indeed entangled, one needs to rule out that there is any decomposition into product states. Answering this question for general density matrices is a non-deterministic polynomial-time (NP)-hard problem[41]. To be precise, even the relaxed problem allowing for a margin of error that is inversely polynomial (in contrast to inversely exponential, as in the original proof by Gurvits) in the system dimension remains NP-hard[42].

Pure states, separable or entangled, admit a Schmidt decomposition into bi-orthogonal product vectors, that is, one can write them as $|\psi\rangle_{AB} = \sum_{i=0}^{k-1} \lambda_i |ii\rangle$. The coefficients $\lambda_i \in \mathbb{R}^+$ are called the Schmidt coefficients. Their squares, which are equal to the eigenvalues of the marginals $\rho_{A/B} := \text{Tr}_{B/A} |\psi\rangle\langle\psi|_{AB}$, are usually arranged in decreasing order and collected in a vector $\vec{\lambda}$ with components $[\vec{\lambda}]_i := \lambda_i^2$. The number k of non-zero Schmidt coefficients is called the Schmidt rank or sometimes the dimensionality of entanglement, as it represents the minimum local Hilbert space dimension required to faithfully represent the correlations of the quantum state. One of the fundamental pillars of state manipulation under LOCC is Nielsen's majorization theorem[39,43]: a quantum state with (squared) Schmidt coefficients $\vec{\lambda}$ can be transformed to another state with Schmidt coefficients $\vec{\lambda}'$ by a LOCC transformation if and only if $\vec{\lambda} \prec \vec{\lambda}'$, that is, the vector of squared Schmidt coefficients of the output state majorizes the corresponding vector of the input state. This also conveniently captures two extremal cases. On the one hand, a separable state has a corresponding vector of (1, 0, …, 0), majorizing every other vector, and thus cannot be transformed into any entangled state by LOCC. On the other hand, in dimensions d, the vector $(\frac{1}{d}, \frac{1}{d}, \ldots, \frac{1}{d})$ is majorized by every other vector. The corresponding state $|\Phi^+\rangle := \frac{1}{\sqrt{d}} \sum_{i=0}^{d-1} |ii\rangle$ can thus be transformed into any other quantum state and is therefore referred to as a maximally entangled state.

Entanglement quantification

Any meaningful entanglement quantifier for pure states is hence a function of the Schmidt coefficients. The two most prominent representatives are the entropy of entanglement, that is, the von Neumann entropy of the marginals, or equivalently the Shannon entropy of the squared Schmidt coefficients $E(|\psi\rangle_{AB}) := S(\rho_{A/B}) = -\sum_{i=0}^{k-1} \lambda_i^2 \log_2(\lambda_i^2)$, and the Rényi zero-entropy or the logarithm of the marginal rank. For mixed states, the fact that there exist infinitely many pure state decompositions complicates the quantification of entanglement. How is one to unambiguously quantify the entanglement of a state that admits different decompositions into states with various degrees of entanglement? A straightforward answer presents itself in the form of an average over the entanglement $E(|\psi_i\rangle)$ within a given decomposition, minimized over all decompositions $\mathcal{D}(\rho)$, that is, $E(\rho) := \inf_{\mathcal{D}(\rho)} \sum_i p_i E(|\psi_i\rangle)$. When the entropy of entanglement is the measure of choice, this convex roof construction leads to the entanglement of formation E_{oF} (REFS[44,45]). Its regularization $\lim_{n\to\infty} \frac{1}{n} E_{\text{oF}}(\rho^{\otimes n})$ has a convenient operational interpretation as the entanglement cost[44,46], the asymptotic LOCC interconversion rate from m two-qubit Bell states $|\psi\rangle^{\otimes m} = \frac{1}{\sqrt{2}}(|00\rangle + |11\rangle)^{\otimes m}$ to n copies of ρ, or $\rho^{\otimes n}$. Conversely, one may define distillable entanglement as the asymptotic LOCC conversion rate from non-maximally entangled states to Bell states[47,48].

If the E_{oF} were additive, it would coincide with the entanglement cost. However, as shown by Hastings[49], the entanglement of formation is only sub-additive. For other measures, such as the Schmidt rank, a more appropriate generalization is to maximize (instead of averaging) over all states within a given decomposition. In this way, the Schmidt number of mixed quantum states, defined as $d_{ent} := \inf_{\mathcal{D}(\rho)} \max_{|\psi_i\rangle \in \mathcal{D}(\rho)} \mathrm{rank}(\mathrm{Tr}_A(|\psi_i\rangle\langle\psi_i|))$[50], directly inherits the operational interpretation of the Schmidt rank for pure states. These are just two examples of generally inequivalent entanglement measures and monotones. For an in-depth review, we refer the interested reader to REFS[17,18]. Whereas these and many other measures have very instructive and operational interpretations, even deciding whether they are non-zero is, in general, an NP-hard problem, even if the density matrix is known to infinite precision. However, not only will uncertainties be associated to the different matrix elements obtained in actual experiments but the sheer amount of information that needs to be collected renders full state tomography too cumbersome to be practical beyond small-scale demonstrations[51,52]. This is exacerbated in the multipartite case, in which the system dimension grows exponentially with the number of parties.

An implication of this observation is that the amount of actual entanglement in a quantum system not only depends on the measure used (and hence the context or task for which it is applied) but also is impossible to ascertain exactly. However, it is possible to certify the presence of and even to provide a lower bound on the amount of entanglement for various useful quantifiers through few experimentally realizable measurements, which is the main focus of this Review.

Partial transposition and entanglement distillation

A recurring feature among entanglement tests is overcoming the hardness of the separability problem by detecting only a subset of entangled states. An example (that nonetheless requires knowledge of the entire density matrix) is the positive partial transpose (PPT) criterion[53,54]. Partially transposing a separable state leads to a positive semi-definite density matrix. However, this need not be the case for entangled states because the partial transposition is an instance of a positive, but not completely positive, map. By contrast, positive maps $\Lambda_P[\rho] \geq 0$ lead to positive semi-definite matrices when applied to positive semi-definite matrices, such as quantum states. Completely positive maps $(\Lambda_{CP} \otimes \mathbb{1}_d)[\rho] \geq 0 \; \forall d \in \mathbb{Z}^+$, on the other hand, lead to positive semi-definite operators even when applied to marginals. In fact, it was proved that a state is separable if and only if it remains positive under all positive maps applied to a subsystem[54].

In addition to serving as an easily implementable entanglement test (provided the density matrix is known), the partial transposition provides a simple sufficient criterion for distillation. As shown in REF.[55], the process of entanglement distillation[47,48], that is, the simultaneous local processing of multiple copies of pairwise distributed quantum states to concentrate the entanglement in one pair, is possible only if there exists at least a 2×2-dimensional subspace of the multicopy state space that is not PPT. Because any tensor products of PPT states are also PPT, this directly implies that even though many PPT states are entangled, none of them are distillable. Conversely, whether all states that are non-positive under partial transposition (NPT) are distillable is still an open problem[56], but it is known that for any finite number of copies, the answer is negative[57].

The PPT map is also commonly used to quantify entanglement through the logarithmic negativity[58], defined as the logarithm of the trace norm of the partially transposed density matrix $\mathcal{N}(\rho) := \log_2(||\Lambda_P[\rho]||_1)$. Loosely speaking, it captures how much the partial transpose fails to be non-negative. The logarithmic negativity is a prominent example of an entanglement monotone[59] (as is the negativity[60,61]), that is, a quantity that is non-increasing under LOCC like any entanglement measure but that does not need to be non-zero for all entangled states.

Whereas calculating the result of applying a positive map requires knowledge of the entire density matrix, it is still possible to harness positive maps to construct powerful entanglement witnesses[54] even if only partial or imprecise information about the state is available. Suppose one is provided with a theoretical target state ρ_T that is not positive semi-definite under a positive (but not completely positive) map Λ_P, $\Lambda_P[\rho_T] \not\geq 0$. Then there exist vectors (for example, preferably the eigenvector $|\psi^-\rangle$ of $\Lambda_P[\rho_T]$ corresponding to the smallest eigenvalue) for which $\langle\psi^-|\Lambda_P[\rho_T]|\psi^-\rangle = \mathrm{Tr}(\Lambda_P[\rho_T]|\psi^-\rangle\langle\psi^-|) < 0$. Through the dual map Λ_P^*, this is equivalent to the statement $\mathrm{Tr}(\rho_T \Lambda_P^*[|\psi^-\rangle\langle\psi^-|]) < 0$, whereas $\mathrm{Tr}(\sigma \Lambda_P^*[|\psi^-\rangle\langle\psi^-|]) \geq 0$ for all separable states σ. The Hermitian operator $\Lambda_P^*[|\psi^-\rangle\langle\psi^-|]$ is thus an example of an entanglement witness (BOX 1), an observable that can, in principle, be measured to detect entangled states, at least in the vicinity of ρ_T. Some illustrative examples of linear and nonlinear (in ρ) entanglement witnesses (negative values detected), positive (but not completely positive) maps (resulting non-positive operators detected) detecting bipartite entanglement for two qubits, maximal entanglement dimensionality (Schmidt number 3) for two qutrits and genuine multipartite entanglement (GME) for three qubits are shown in TABLE 1. The exemplary techniques detect the entanglement, Schmidt number or GME for the generalized state $|\psi\rangle = \frac{1}{\sqrt{d}} \sum_{i=0}^{d-1} |i\rangle^{\otimes n}$ for $(n, d) = (2, 2), (2, 3)$ and $(3, 2)$, respectively.

Beyond linear witnesses

To improve over linear witnesses, a very useful experimentally applicable method makes use of local uncertainty relations (LURs). The idea to derive entanglement criteria by means of LURs has some analogies with the original Einstein–Podolsky–Rosen (EPR)–Bell approach in the sense that it considers pairs of non-commuting single-party observables, say (A_1, A_2) for party A and (B_1, B_2) for party B. Because the A_i do not commute with each other, their uncertainties cannot both be zero simultaneously. The same is true for the B_i. However, in the joint system, the uncertainties of the collective observables

Box 1 | **Entanglement witnesses**

Entanglement witnesses[206] are one of the most important practical entanglement certification techniques. The set $\mathcal{S}$ of separable states is a convex subset of all quantum states. The Hahn–Banach theorem guarantees that there exists a hyperplane for every entangled state ρ that separates this state from the separable set. These hyperplanes correspond to observables W, such that $\mathrm{Tr}(W\rho)<0$, whereas $\mathrm{Tr}(W\sigma)\geq 0$ for all $\sigma\in\mathcal{S}$. Measurements of such entanglement witness operators can hence certify the presence of entanglement: having identified an operator W whose expected value is non-negative for all separable states, measuring $\langle W\rangle_\rho$ and obtaining a negative value conclusively demonstrates that ρ is entangled. Although such witnesses exist for every entangled state ρ, finding $\langle W\rangle_\rho\geq 0$ does not imply that ρ is separable; W might simply not be a suitable witness for the underlying state. The challenge hence lies in the construction of useful entanglement witnesses. Without specific information about the state produced in an experiment, this is a formidable task. However, when the underlying state can be expected to be close to a target state $|\psi_T\rangle$, there exists a canonical witness construction, given by

$$W := \lambda_{\max}^2 \mathbb{1} - |\psi_T\rangle\langle\psi_T|$$

Here, $\lambda_{\max}$ is the largest Schmidt coefficient of $|\psi_T\rangle$, representing the maximal overlap of any separable state with $|\psi_T\rangle$, such that $\max_{\sigma\in\mathcal{S}}\mathrm{Tr}(\sigma W)=0$.

Whereas entanglement witnesses are observables and can hence, in principle, be evaluated by measurements in only a single basis, the corresponding basis cannot be a product basis but must consist (at least in part) of basis states featuring entanglement across the partition for which entanglement is to be detected in the first place. More specifically, we can express any witness W for entanglement across a bipartition $A|B$ with respect to local operator bases $\{g_A^i\}_i$ and $(g_B^j)_j$ (for example, appropriately normalized Pauli matrices for qubits) with $\mathrm{Tr}(g_{A/B}^i g_{A/B}^j)=d\delta_{ij}$, that is, $W=\sum_{i,j}c_{ij}g_A^i\otimes g_B^j$. This means that entanglement witnesses can also be obtained by a larger number of local measurements, in which the crucial figure of merit is the number of non-zero coefficients c_{ij}, determining the overall number of local measurement settings required to evaluate the witness.

In the figure, the schematic on the left-hand side shows the nested convex structure of a 3×3-dimensional Hilbert space, the set of separable states $\mathcal{S}$ (with Schmidt number $k=1$, blue), the set of states positive under partial transposition (PPT, containing $\mathcal{S}$), the set of states with Schmidt number $k\leq 2$ (green, containing PPT entangled states for which $k=2$) and the set of states with Schmidt number $k\leq 3$ (yellow, containing all other states). The entanglement witness W shown is an example for a Schmidt number witness, certifying genuine 3D entanglement. In the figure, the schematic on the right-hand side shows the nested convex structure of multipartite entanglement in a three-party Hilbert space, showing the set of fully separable states ($\mathcal{S}_3$, blue), biseparable states ($\mathcal{S}_2$, green) and genuine multipartite entanglement (GME, yellow). The entanglement witness W shown is an example of a multipartite entanglement witness certifying genuine three-partite entanglement.

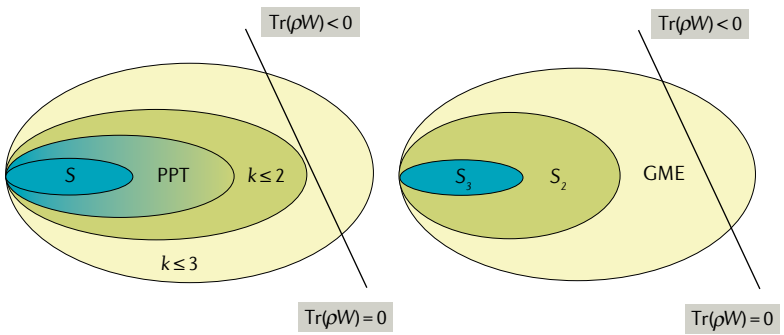

$M_i=A_i\otimes\mathbb{1}+\mathbb{1}\otimes B_i$ can both vanish at the same time, provided that the state is entangled.

A powerful and instructive example is given in terms of the variance $(\Delta A)_\rho^2=\mathrm{Tr}(A^2\rho)-\mathrm{Tr}(A\rho)^2$. The sum $(\Delta A_1)_{\rho_A}^2+(\Delta A_2)_{\rho_A}^2\geq U_A$ must have a non-zero lower bound $U_A>0$ for all single-party states ρ_A whenever the two observables do not commute. Similarly, $(\Delta B_1)_{\rho_B}^2+(\Delta B_2)_{\rho_B}^2\geq U_B$ for all ρ_B. Thus, by simple concavity arguments, one can prove that $(\Delta M_1)_{\rho_{AB}}^2+(\Delta M_2)_{\rho_{AB}}^2\geq U_A+U_B$ must hold for all separable states $\rho_{AB}=\sum_k p_k(\rho_A\otimes\rho_B)_k$ (REFS[62–65]). This method hence combines two conceptual features: first, the LURs themselves — representing a trade-off between information about different complementary (non-commuting) observable quantities — and second, the fact that those (nonlinear) quantities are either concave or convex. Thus, analogous reasoning can be applied to other quantifiers of uncertainty, for instance, the quantum Fisher information, introduced in the context of quantum metrology and proved to be related to metrological applications of entanglement[34]. In addition, LURs in the form of a product of uncertainties (variances) can be used (although requiring a somewhat more complicated mathematical treatment) to derive entanglement criteria resembling Heisenberg uncertainty relations in their original formulation[66–68].

It is also worth mentioning that all nonlinear entanglement witnesses arising from sums of variances can be cast in a compact form in terms of the covariance matrix $\Gamma_{ij}(\rho)=\frac{1}{2}\langle g_ig_j+g_jg_i\rangle_\rho-\langle g_i\rangle_\rho\langle g_j\rangle_\rho$ of a local basis of observables. The resulting covariance matrix criterion[69,70] was proved to be necessary and sufficient for the special case of two qubits, provided that one makes use of local filterings that map the state to its filtered normal form (FNF) $\rho\mapsto\rho_{\mathrm{FNF}}:=(F_A\otimes F_B)\,\rho\,(F_A\otimes F_B)^\dagger$ such that $\rho_{\mathrm{FNF}}=\frac{1}{4}(\mathbb{1}_4+\sum_{i,j=x,y,z}t_{ij}\sigma_i\otimes\sigma_j)$, where σ_k ($k=x,y,z$) are the Pauli matrices. For local dimensions larger than two, the covariance matrix criterion can, in principle, be evaluated using semi-definite programmes, but in its general form, this is still a difficult task, even for bipartite systems.

Bounding witnessed entanglement

When using an approach based on witnesses, one is also interested in quantitative statements about the detected entanglement based on the data of the (preferably) few measurements required for the witness itself. A simple yet general method to compute lower bounds on convex functions of quantum states $E(\rho)$ (such as entanglement measures) using only a few expectation values is based on Legendre transforms[71,72]. In this context, let us define such a transform as $\hat{\mathrm{E}}(W):=\sup_\rho[\mathrm{Tr}(W\rho)-E(\rho)]$, where the supremum is taken over quantum states ρ. Note that for a given convex function $E(\rho)$, the quantity $\hat{\mathrm{E}}(W)$ depends only on the chosen witness W. Then, a tight lower bound on $E(\rho)$ for the underlying (unknown) system state ρ is obtained through another Legendre transformation, which leads to

$$E(\rho)\geq\sup_\lambda[\lambda\,\mathrm{Tr}(W\rho)-\hat{\mathrm{E}}(\lambda W)] \qquad (2)$$

where λ is real and $\mathrm{Tr}(W\rho)$ is obtained from measurements. The applicability of this technique largely depends on whether $\hat{\mathrm{E}}(W)$ (and hence $E(\rho)$ for a given ρ) can be efficiently computed, but this technique has turned out to be a powerful tool to quantify multipartite entanglement based on uncertainty relations[73–76]. Another option is a direct construction of witnesses

Table 1 | **Examples of entanglement detection methods**

	Witness $\mathrm{Tr}(\rho W)\geq 0$	Nonlinear witness $f(\rho)\geq 0$	Positive map $\Lambda[\rho]\geq 0$
Two qubits	$-\mathrm{Re}(\langle 00\vert\rho\vert 11\rangle)+\frac{1}{2}(\langle 01\vert\rho\vert 01\rangle+\langle 10\vert\rho\vert 10\rangle)$	$\sqrt{\langle 01\vert\rho\vert 01\rangle\langle 10\vert\rho\vert 10\rangle}-\vert\langle 00\vert\rho\vert 11\rangle\vert$	$\rho\mapsto\rho^{T_A}$
Two qutrits	$\frac{2}{3}-\frac{2}{3}\mathrm{Re}(\langle 00\vert\rho\vert 11\rangle+\langle 00\vert\rho\vert 22\rangle+\langle 11\vert\rho\vert 22\rangle)$ $-\frac{1}{3}(\langle 00\vert\rho\vert 00\rangle+\langle 11\vert\rho\vert 11\rangle+\langle 22\vert\rho\vert 22\rangle)$	$\det(M)$ with $M_{ij}=\frac{1}{2}[2\delta_{ij}\langle i\vert\rho_B\vert j\rangle-\langle ii\vert\rho\vert jj\rangle]$	$\rho\mapsto\mathbb{1}_3\otimes\rho_B-\frac{1}{2}\rho_{AB}$
Three qubits	$-\mathrm{Re}(\rangle 000\vert\rho\vert 111\rangle)$ $+\frac{1}{2}(\langle 001\vert\rho\vert 001\rangle+(\langle 110\vert\rho\vert 110\rangle)$ $+\frac{1}{2}(\langle 010\vert\rho\vert 010\rangle+(\langle 101\vert\rho\vert 101\rangle)$ $+\frac{1}{2}(\langle 100\vert\rho\vert 100\langle+(\langle 011\vert\rho\vert 011\rangle)$	$-\vert\langle 000\vert\rho\vert 111\rangle\vert+\sqrt{\langle 001\vert\rho\vert 001\rangle\langle 110\vert\rho\vert 110\rangle}$ $+\sqrt{\langle 010\vert\rho\vert 010\rangle\langle 101\vert\rho\vert 101\rangle}+\sqrt{\langle 100\vert\rho\vert 100\rangle\langle 011\vert\rho\vert 011\rangle}$	$\rho\mapsto\mathbb{1}+\sigma_x^A\rho^{T_A}\sigma_x^A$ $+\sigma_x^B\rho^{T_B}\sigma_x^B+\sigma_x^C\rho^{T_C}\sigma_x^C$

The symbol ρ denotes density operators, whereas $\langle i\vert\rho\vert j\rangle$ denotes density matrix elements. W denotes a witness operator and f and Λ indicate maps from density operators to positive numbers or positive semi-definite operators, respectively. The quantities σ_x^i represent the usual Pauli-x operator for party i. The table presents some illustrative examples of linear and nonlinear (in ρ) witnesses (negative values detected), positive (but not completely positive) maps (resulting non-positive operators detected) detecting bipartite entanglement for two qubits, maximal entanglement dimensionality (Schmidt number 3) for two qutrits and genuine multipartite entanglement (GME) for three qubits. All the exemplary techniques detect entanglement, Schmidt number or GME for the generalized state $\vert\psi\rangle=\frac{1}{\sqrt{d}}\sum_{i=0}^{d-1}\vert i\rangle^{\otimes n}$ for $(n, d)=(2, 2)$, $(2, 3)$ and $(3, 2)$, respectively.

that have a natural connection between their expectation value and a suitably chosen entanglement measure[77–79].

Measurement strategies and restrictions

Identifying measurement strategies

The previous discussion of bipartite entanglement showcases one of the central challenges for experimental verification: entanglement quantification and detection methods are available in abundance but are often defined in a formal way. Some allude to observable quantities, some to maps on density matrices and others to positive operator-valued measures (POVMs). Identifying the most suitable and efficient practical method for a specific experimental setup is hence not straightforward. For instance, the types of measurements that can be most easily (or at all) implemented depend on the experimental platform, and their identification and comparison may be obfuscated by varying terminologies. A consistent challenge across all platforms and paradigms is the exponential number of potential measurements that could be required for the desired task. Moreover, this number is often specified in terms of different quantifiers, such as the number of global settings, the number of local settings, the number of observables or the number of density matrix elements. To provide a comparative overview of the complexity of different detection methods, we give more precise definitions, briefly review some practical methods of data acquisition and identify which tests work well with what type of data.

Formally, all measurements can be described by POVMs, that is, sets of positive semi-definite operators $M_i\geq 0$ with the property $\sum_{i=1}^{m} M_i=\mathbb{1}_d$, where m is the number of distinguishable outcomes labelled by i. A special case is the projective measurement, where $M_i=\vert v_i\rangle\langle v_i\vert$ for all i and $m=d$. Each POVM can be thought of as a projective measurement on a larger system, and most experimental implementations indeed work directly with projective measurements. Repeated projective measurements allow estimation of the expectation values $\mathrm{Tr}(\rho M_i)=\langle v_i\vert\rho\vert v_i\rangle$, that is, a complete set of diagonal density matrix elements with respect to a specific basis $\{v_i\}_i$, and, in turn, the expected values of all observables of the form $O=\sum_i\lambda_i\vert v_i\rangle\langle v_i\vert$.

Local versus global

It is useful to distinguish between different types of projective measurements. Most importantly, one differentiates between local and global measurement bases (or observables) depending on whether the basis vectors $\vert v_i\rangle$ are product states $\vert v_i\rangle_{AB}=\vert u_i\rangle_A\otimes\vert w_i\rangle_B$ with respect to the chosen bipartition $A\vert B$ or not. Here, the choice of basis $\{\vert v_i\rangle_{AB}\}_i$ is referred to as a global setting, whereas bases $\{\vert u_i\rangle_A\}_i$ and $\{\vert w_j\rangle_{B_j}$ are called local settings. In the standard scenario for quantum communication, whenever the constituents of the quantum system are spatially separated, local (product basis) measurements are the only possible measurements. In this case, detection, certification or quantification of entanglement requires the measurement of (at least some) off-diagonal density matrix elements. These can be obtained by measurements of diagonal matrix elements of specific (product) bases conjugate with respect to the original basis. Alternatively, it is often useful to work directly with a local operator basis. That is, the Bloch picture can be extended to d-dimensional systems (qudits) and any number of parties in terms of a generalized Bloch decomposition[80] by expanding a quantum state in a basis of suitable matrices g_i, $\rho=\sum_{i_1,i_2,\ldots,i_n=0}^{d^2-1}\rho_{i_1 i_2\ldots i_n}g_{i_1}\otimes g_{i_2}\otimes\cdots\otimes g_{i_n}$. For instance, for two qudits and an operator basis that includes the identity, one has

$$\rho=\frac{1}{d^2}(1_{d^2}+\vec{v}_A\vec{\sigma}\otimes 1_d+\vec{v}_A 1_d\otimes\vec{\sigma}+\sum_{i,j}t_{ij}\sigma_i\otimes\sigma_j),\tag{3}$$

where $\{\sigma_i\}_i$ is a basis of the SU(d) algebra. The Bloch coefficients themselves are obtained as expectation values of local observables, $t_{ij}=\langle\sigma_i\otimes\sigma_j\rangle_\rho$, making the Bloch basis a convenient expression of quantum states only in terms of results of local measurements instead of abstract density matrix elements. Whereas, in general, there exist d^2-1 orthogonal generators of SU(d), requiring a large amount of observables to be measured for tomographic purposes (the g_i generally do not have full rank), most of them can be represented through dichotomic operators and are

thus often easier to implement than multi-outcome measurements. In contrast to any local measurements, probes interacting with multiple constituents of the system simultaneously or global observables whose eigenstates do not factorize (such as the magnetization) can give rise to entangling measurements. These measurements are inherently global, and the individual detector events can be used directly to estimate the correlators necessary for measuring entanglement witnesses. This is particularly relevant experimentally when the number of involved parties becomes very large, $n \approx 10^3$–10^{12} or larger, in which case a reconstruction of the full density matrix is prevented by the extremely large number of required measurements. At the same time, it is typically possible to measure level populations and consequently infer moments of N-particle collective operators such as $J_k = \sum_{i=1}^{n} j_k^{(i)}$. Such quantities are, in turn, directly related to interparticle correlations, potentially providing information about entanglement.

Multi-outcome versus single outcome

Measurements in any basis may be classified by the method by which the relative frequencies of different measurement outcomes are recorded. In multi-outcome measurements, the interaction of a measurement device with a single copy of the measured system described by ρ provides one of several (ideally one of d) different outcomes i associated with the projection into $|v_i\rangle$. That is, the detector event may fall into one of d categories that can be distinguished by the experimenter. After N such rounds of multi-outcome measurements, each resulting in one detector event, the outcome i is obtained S_i times, such that $\sum_{i=1}^{d} S_i = N$, and the expected value of M_i is estimated to be $\mathrm{Tr}(M_i\,\rho) \approx S_i/N$. However, in single-outcome measurements, filters are used to select only one particular outcome i, for which the detector (such as a photodetector placed behind a polarization filter) responds with a 'click'. In principle, one may think of a 'no click' event as a second outcome, but this works only if the imminent event is heralded. A much simpler alternative is usually to collect the number S_i of clicks in the filter setting i during some fixed integration period and again associate $\langle v_i|\,\rho\,|v_i\rangle \approx S_i/N$ with $N = \sum_{i=1}^{d} S_i$ for the chosen orthonormal basis $\{|v_i\rangle\}_i$. For non-orthonormal bases, this approach can still be used with minor modifications[81]. Crucially, the data corresponding to a d-outcome measurement can also be obtained from d individual single-outcome measurements. In principle, this also applies to local measurements. For instance, diagonal density matrix elements with respect to the product basis $\{|u_i\rangle_A \otimes |w_j\rangle_B\}_{i,j=1}^{d}$ in a $d \times d$-dimensional Hilbert space can be obtained using d^2 pairs of local filter settings, provided that local detection events for filter settings i and j fall within a sufficiently close time interval to be combined to 'coincidences' $C_{i_A j_B}$. More generally, for n parties, temporal coincidence allows association of the localized single events at n detectors into coincidences $C_{i_1 i_2 \ldots i_n}$ and global density matrix elements $\langle i_1 i_2 \ldots i_n\,|\,\rho\,|\,i_1 i_2 \ldots i_n\rangle = C_{i_1 i_2 \ldots i_n} / \sum_{i_1, i_2, \ldots, i_n} C_{i_1 i_2 \ldots i_n}$.

Statistical error and finite data

The discussion above illustrates that the number of measurement settings required for entanglement tests depends not only on the chosen theoretical method but also on what is counted, such as local or global bases and operators, filter settings (single outcome), dichotomic observables (two outcomes, such as for Bloch decompositions) or multi-outcome measurements. However, regardless of the method used, each single measurement setting still requires a number of repetitions of individual measurements to ensure the desired statistical confidence in the result. That is, the association $\mathrm{Tr}(M_i\,\rho) \approx S_i/N$ is exact only in the limit of infinitely many repetitions, and any real experiment using a finite number of measurements may estimate only probabilities or expected values from frequencies of occurrence of certain measurement outcomes. The confidence in these estimates is then guaranteed by a sufficiently large sample size (number of repetitions). How many samples can be taken with reasonable effort and time largely depends on the specific experimental setup. For instance, whereas many thousands of coincidences can be recorded every second in photonic setups used in communications and the resulting statistical error can be easily computed and does not heavily influence the conclusions drawn, state preparation in other systems is often tedious and not straightforwardly repeatable. In such scenarios, statistical errors and sufficiently narrow confidence intervals become prominent challenges that have to be addressed. Certifying entanglement with finite data was first addressed with simulated two-qubit data[82], but similar reasoning also applies to methods directly aimed at state estimation[83,84]. In this context, REF.[85] also provides a cautionary tale against density matrix reconstruction techniques, as neglecting errors can lead to a systematic overestimation of entanglement and underestimation of fidelity (maximum likelihood reconstructions have thus recently been deemed inappropriate for fidelity estimation[86]). In general, different measurement techniques come at different experimental cost for entanglement estimation or state tomography. This cost can be quantified in the number of states needed for achieving statistical certainty (see, for instance, REF.[87] for optimal strategies in the bipartite case). Nonetheless, if enough repetitions for meaningful statistics are possible (for example, for down-converted photons), the number of different measurement bases and settings remains the principal measure of efficiency. An overview of this figure of merit for the most common measurement strategies is shown in TABLE 2.

Key challenges

High-dimensional entanglement

Entanglement dimensionality. High-dimensional Hilbert spaces enable an encoding of more bits per photon and thus promise increased communication capacities over quantum channels. However, if the security of these channels is to be ensured by entanglement, a major challenge is the certification of high-dimensional entanglement because it should be done with as few measurements as possible and without introducing unwarranted assumptions that may lead to exploitable loopholes in

Table 2 | **Minimal number of measurement settings**

Measurement strategy	Full state tomography	$F(\rho, \Phi)$	$\mathrm{Tr}(\rho W)$
Global observables O	d^n+1	1	1
Collective observables $O=\sum_i o_i \otimes \mathbb{1}_i$	$\leq(d+1)^n$	NA	2
Bi-product bases (local MUB) $\mathrm{eig}(O)=\{\otimes_{i=1}^2 \lvert v_i\rangle\}$	$(d+1)^2$	$d+1$	2
Product bases (local MUB) $\mathrm{eig}(O)=\left\{\otimes_{i=1}^n \lvert v_i\rangle\right\}$	$(d+1)^n$	$\leq(d+1)^n$	2
Bi-product Bloch bases $O=\sigma_1^{j_1}\otimes\sigma_2^{j_2}$	$(d^2-1)^2$	d^2-1	2
Product Bloch bases $O=\otimes_{i=1}^n \sigma_i^{j_i}$	$(d^2-1)^n$	$\leq(d^2-1)^n$	2
Local filters $O=\otimes_{i=1}^n \lvert v_i\rangle\langle v_i\rvert$	$(d(d+1))^n$	$(d+1)d^n$	$2d^n$

The table shows the minimal number of required measurement settings as a function of Hilbert space dimension d for different commonly used measurement strategies to perform full state tomography, optimal estimation of fidelity with respect to pure target states Φ [$F(\rho, \Phi) := \langle\varphi|\rho|\varphi\rangle$] or evaluation of an entanglement witness for 2 or n d-dimensional subsystems. Global observables can be used for optimal tomography based on mutually unbiased bases (MUBs)[259] to estimate the fidelity via the observable $O=\Phi=|\varphi\rangle\langle\varphi|$ or directly represent entanglement witnesses $O=W$. Collective observables are (weighted) averages of single-party observables that can be used to witness entanglement via their second moments (or alternatively, if the second moments of a single observable are given by a weighted sum of local observables, in which terms are local but may act nontrivially on more than one subsystem — for an interaction Hamiltonian, for example — then it is already sufficient to certify entanglement[195,196]). Local (bipartite or n-partite) measurements in MUBs (or tilted bases[81]) can be used for local tomography and direct fidelity estimation (or for certifying a lower bound with only two product bases[81]). Determining the coefficients of the Bloch decomposition requires the measurement of all d^2-1 local Bloch vector elements in every possible combination. Two anti-commuting operators, however, are already sufficient for constructing entanglement witnesses in bipartite[260] and multipartite systems[261,262]. Post-selecting coincidence counts in a single-outcome scenario (such as filtering) requires every possible projection on a tomographically complete set of states, for instance, d^n measurement settings to measure in a single basis (although it is possible to detect entanglement without even knowing a single density matrix element[263]).

the certification. In this context, matrix completion techniques[88,89], semi-definite programmes[89,90], uncertainty relations[91] and mutually unbiased bases[81,92,93] provide versatile tools for quantifying high-dimensional entanglement in different contexts.

The canonical witnesses for known target states $|\psi_T\rangle$ shown in BOX 1 can readily be generalized to detect high-dimensional entanglement in the same way. One defines $W_k := \sum_{i=1}^k \lambda_i^2 \mathbb{1} - |\psi_T\rangle\langle\psi_T|$, where $\sum_{i=1}^k \lambda_i^2$ denotes the sum over the k largest squared Schmidt coefficients of the target state[94]. Whereas this witness faithfully certifies high-dimensional entanglement of any pure target state, it is decomposable (for instance, it detects only NPT states) and features a weak resistance to noise. However, it requires only an estimate of the target state fidelity, which can be efficiently obtained with few measurements[81,87].

High-dimensional entanglement can also be ascertained using suitable quantitative measures. For instance, certifying an entanglement of formation beyond $\log_2(k)$ also implies $(k+1)$-dimensional entanglement. Alternatively, high-dimensional entanglement can also be quantified directly by the g-concurrence[95], the bounds for which can be obtained from nonlinear witness operators[96].

From a local Hilbert space perspective, multiple copies of entangled qubit pairs can be considered as equivalent to high-dimensionally entangled systems. However, this equivalence breaks down for distributed quantum systems; that is, genuine high-dimensionally entangled systems can feature correlations that are, in principle, unattainable by multiple copies of two-qubit entangled states[97], which has recently been used in a photonic experiment to verify genuine high-dimensional entanglement[98].

Besides practical challenges, many open questions still remain concerning the mathematical structure of high-dimensional entanglement. Whereas it is known to generically occur in high-dimensional Hilbert spaces[99], few techniques are known for constructing witnesses detecting PPT entanglement in high dimensions (or, dual to that problem, non-decomposable k-positive maps[54]). Even among PPT states, high-dimensional entanglement is generic[100] but, at the same time, not maximal[101].

Photonic high-dimensional entanglement. Photonic systems, which are inherently multimode in the temporal and spatial degrees of freedom, naturally lend themselves to the creation and measurement of high-dimensional entanglement. Here, we discuss some landmark experiments and accompanying theoretical techniques used for demonstrating the high-dimensional entanglement of two photons in their orbital angular momentum (OAM), transverse spatial position–momentum, time–frequency and path degrees of freedom.

The high-dimensional entanglement of two photons in the spatial or temporal degrees of freedom usually results from the conservation of energy and momentum in a second-order nonlinear process, such as spontaneous parametric down-conversion. This process entails the annihilation of one pump photon with energy $\hbar\omega$ and zero OAM in a nonlinear crystal, resulting in the creation of two daughter photons with energy $\frac{1}{2}\hbar\omega$. Whereas formally the dimension of the Hilbert space relating to modal properties is infinite, only a finite number of modes will be populated significantly. Thus, the effective dimensionality of the resulting two-photon state depends on the spectral and spatial properties of the pump beam, as well as on the phase-matching function governing the nonlinear process. For example, the width of the pump beam and the length of the nonlinear crystal determine the dimensionality of an OAM-entangled state[102].

Some of the first demonstrations of high-dimensional entanglement were performed with photons entangled in their OAM, which is a discrete quantum property resulting from a spatially varying amplitude and phase distribution[103,104]. This type of entanglement was first demonstrated with Schmidt number $d_{ent}=3$ in an experiment that measured a generalized Bell-type inequality[105] with single-outcome, holographic projective filters that allowed the measurement of coherent superpositions of OAM at the single-photon level[106]. In recent years, the development of computer-programmable wavefront-shaping devices, such as spatial light modulators, has allowed the measurement of OAM-entangled states with ever-increasing dimension. Examples of such experiments include the certification of $d_{ent}=100$ spatial-mode entanglement with a visibility-based entanglement witness[107] and $d_{ent}=11$ OAM-entanglement with a generalized Bell-type test[108], both with certain assumptions on the state. More recently, an assumption-free

entanglement witness was implemented with spatial light modulators certifying $d_{ent} = 9$ OAM entanglement with only two measurement settings[81].

A natural second basis for observing high-dimensional entanglement is found in the transverse photonic position–momentum degrees of freedom. A discretized version of the transverse position can be thought of as a 'pixel' basis, which is particularly relevant today with the development of sensitive single-photon cameras. Pixel entanglement was first observed with arrays of three and six fibres[109], and entanglement was certified by violating the EPR–Reid criterion[66] by setting a lower bound on the product of conditional variances in position and momentum: $\Delta^2(\rho_1 - \rho_2)\Delta^2(p_1 + p_2) \geq \frac{\hbar^2}{4}$. More recently, electron-multiplying cameras that exhibit a high single-photon detection efficiency have been used to violate the EPR–Reid criterion by very high values, albeit by subtracting a large, uncorrelated background[110,111]. Other approaches that aim to reduce the number of measurements required to certify position–momentum entanglement have been developed, such as using compressed-sensing techniques to measure such states in a sparse basis[112] or employing periodic masks to increase photon-counting rates[113].

It is important to note here that in several experimental works, the term Schmidt number is used to define a different concept than the canonical one mentioned in the introduction. This surrogate quantity refers to the inverse purity, which for pure states is related to the Schmidt coefficients via $\mathrm{PR}(|\psi\rangle) = (\Sigma_i \lambda_i^4)^{-1}$ and is supposed to roughly quantify the number of local dimensions that relevantly contribute to the observed coincidences. This approach was introduced[114] to describe pure continuous-variable systems, in which the Schmidt rank of pure two-mode squeezed states is infinite while any proper entanglement entropy is still finite (in particular, the inverse purity is the exponential of the Rényi-2 entropy of entanglement).

The development of silicon integrated photonic circuits presents another versatile platform for high-dimensional entanglement, in which quantum states are simply encoded in different optical paths of a circuit. Whereas such circuits have been used extensively for quantum information processing with qubits[115,116], their first implementation for qutrit entanglement was demonstrated only recently, with integrated multiport devices enabling the realization of any desired local unitary transformation in a two-qutrit space[117]. A more recent experiment certified up to $d_{ent} = 14$ through the use of nonlinear device-independent dimension witnesses in a large-scale 16-mode photonic integrated circuit and demonstrated violations of a generalized Bell-type inequality[105] and the recently developed Salavrakos–Augusiak–Tura–Wittek–Acín–Pironio (SATWAP) inequality[118] in up to $d_{ent} = 8$ (REF.[119]).

Alongside position–momentum encoding, the time–frequency domain presents yet another powerful platform available for the investigation of high-dimensional entanglement. Early experiments in this direction demonstrated high-dimensional entanglement in photonic time bins generated by spontaneous parametric down-conversion with a mode-locked, pulsed pump laser[120,121]. A central challenge in certifying time-bin entanglement is measuring coherent superpositions of multiple time bins. Usually performed with unbalanced interferometers, this method can measure only a single 2D subspace at a time and faces problems of scalability and stability. A recent experiment overcame these problems through the use of matrix completion methods that required only coherent superpositions of adjacent time bins in order to certify $d_{ent} = 18$ entanglement with 4.1 ebits of entanglement of formation[89]. In parallel, experiments certifying high-dimensional frequency-mode entanglement have also been demonstrated, for example, by the manipulation of broadband spontaneous parametric down-conversion through spatial light modulators[122] or through electro-optic phase modulation of photons generated by spontaneous four-wave mixing in integrated micro-ring resonators[123]. Finally, multiple photonic degrees of freedom can be combined to produce what is referred to as hyperentanglement. This was first demonstrated with photonic OAM, time–frequency and polarization, in which entanglement was certified in each degree of freedom through a Bell Clauser–Horne–Shimony–Holt test[124]. More recently, a hyperentangled state of polarization and energy–time was transmitted over 1.2 km of free space, and high-dimensional entanglement in $d_{ent} = 4$ was certified through an entanglement witness relating visibility to state fidelity[90].

In addition to photonic systems, high-dimensional quantum states have been realized in other systems, such as Caesium atoms[125], transmon superconducting qubits[126] and nitrogen vacancy centres[127]. Recent progress has also been made on entangling two micromechanical oscillators consisting of nanostructured silicon beams[128]. Matter-based systems such as these may provide yet another playground for exploring the types of complex entanglement achieved thus far only with photonic systems.

Multipartite entanglement

Applications of multipartite entanglement. The controlled generation and manipulation of multipartite entangled states are big challenges in current experiments. Multipartite entangled states feature across different disciplines, and thus our Review cannot do justice to the complexity of this topic. To name just a few, multipartite entanglement forms the basis for quantum networking proposals in quantum communication[129–132], it is a key resource for beating the standard quantum limit in quantum metrology[133], it is important in quantum error correcting codes[134], and it appears as a generic ingredient in quantum algorithms[135] and as the principal resource in measurement-based quantum computation[136]. The latter two topics motivated the introduction of quantum states representable by graphs[137] or hypergraphs[138]. As these are locally equivalent to so-called stabilizer states, the two concepts are often used synonymously and a lot of effort has been invested in certifying entanglement for stabilizer states[139,140].

Furthermore, apart from practical, technologically oriented applications, (multipartite) entanglement is closely connected to important physical phenomena, from the physics of many-body systems to quantum thermodynamics and quantum gravity. In thermodynamics,

the entanglement of many-body systems is a crucial ingredient for reaching thermodynamic equilibrium[141], whereas the growth of entanglement entropies with subsystem areas or volumes is of high importance in the field of condensed-matter physics[26,28]. The entanglement of thermal states is drastically influenced by quantum criticality: a high degree of entanglement appears in ground states across a quantum phase transition, with a scaling law that depends on the universality class of the transition. Thus far, theoretical studies in this framework have been devoted to entanglement across bipartitions, especially in ground states (quantified by the concurrence of two sites crossing the partition or the von Neumann entropy of a block), as well as to multipartite entanglement in thermal states (with criteria arising from collective quantities)[20,142]. In the former case, the area law of entanglement for non-critical systems emerged as a major result together with the corresponding classification of entangled states as tensor networks, a notion closely connected to classical simulability of many-body states[26–28].

Given the different types of entanglement that can exist between multiple constituents and the different physical platforms, approaches to entanglement certification vary. First, we overview a selection of theoretical techniques and then provide examples of their application in few-body systems, such as photons and ion traps (BOXES 2 and 3, respectively), and many-body systems, such as atomic gases (BOX 4), noting that other promising realizations of multipartite entanglement exist (for instance, using superconducting qubits[143,144]), but their detailed description goes beyond the scope of this Review.

Genuine multipartite entanglement. The definitions for entanglement across bipartitions of the systems straightforwardly carry over to the many-particle case, but there is a much deeper structure underlying the potential ways in which multipartite systems can be entangled. To unravel this structure, we revisit the definition of separability. There exist states of multipartite systems that can be factored into tensor products of multiple parts. This leads to the definition of k-separable pure states as $|\Psi_{k-\mathrm{sep}}\rangle := \bigotimes_{i=1}^{k} |\Phi_{\alpha_i}\rangle$, where the $\alpha_i \subseteq \{1, 2, \cdots, N\}$ refer to specific subsets of systems in the collection of N parties, that is, $\bigcup_{i=1}^{k} \alpha_i = \{1, 2, \cdots, N\}$ and $\alpha_i \cap \alpha_j = \varnothing \forall i \neq j$. States for which $k = N$ are called fully separable, as there is no entanglement in the system. In the other extreme of $k = 1$, states are called multipartite entangled, because for all possible partitions of the system, one finds entanglement. Considering general (mixed) quantum states adds another layer of complexity to this notion, as k-separability has to be defined as $\rho_{k-\mathrm{sep}} := \sum_i p_i |\Psi^i_{k-\mathrm{sep}}\rangle\langle\Psi^i_{k-\mathrm{sep}}|$, where each of the $|\Psi^i_{k-\mathrm{sep}}\rangle$ can be separable with respect to a different k-partition. Whereas states with $k = N$ are still fully separable and can be prepared purely by LOCC, the case of $k = 1$ is referred to as genuine multipartite entanglement. Here, the word genuine emphasizes the fact that the state indeed cannot be prepared by LOCC without the use of multipartite entangled pure states. Hence, in contrast to the pure state case, there exist density matrices that are entangled across every partition and yet do not require multipartite entanglement for their creation.

Entanglement depth. Whereas the above definition reveals one aspect of entanglement in multipartite systems, it is far from a complete characterization. Consider the two states $|\psi_1\rangle \otimes |\psi_{234}\rangle$ and $|\psi_{12}\rangle \otimes |\psi_{34}\rangle$. Both are 2-separable, yet one describes a tripartite entangled system decoupled from a fourth party, whereas the other represents a pair of independent bipartite entangled states. The concept of entanglement depth attempts to capture this distinction, quantifying the number of entangled subsystems in a multipartite state. In the above example, the entanglement depths would be three and two, respectively. Analogous to GME, the generalization to mixed states makes use of a contrapositive: a state is called k-producible if it can be decomposed as a mixture of products of k-particle states, $\rho_{k-\mathrm{prod}} = \sum_i p_i (\rho_{\beta_1} \otimes \ldots \otimes \rho_{\beta_M})_i$, where the ρ_{β_m} are states of at most k parties. By contrast, a state that is not k-producible has a depth of entanglement of at least $k + 1$ (REFS[73,145]). The two notions of k-separability and k-producibility are hence quite different but match in the extremal cases: a fully separable state is also 1-producible, whereas a genuine N-partite entangled state also has an entanglement depth of N (that is, it is N-producible but not $(N-1)$-producible). The concept of entanglement depth is particularly useful for systems with a large number of particles, that is, approaching the thermodynamic limit, because the resulting hierarchy is (somewhat) independent of the total number of particles N. Entanglement depth is therefore often used in experiments with atomic ensembles[146].

Tensor rank and Schmidt rank vectors. In contrast to the bipartite case, for multipartite systems, there is no such thing as a Schmidt decomposition (at least not in the same sense). That is, not every multipartite state can be written as $|\Psi_N\rangle = \sum_i \lambda_i |i\rangle^{\otimes N}$. Nonetheless, there are two prominent ways to generalize the Schmidt rank for multipartite pure states. The first is the tensor rank r_T, which is defined as the minimum number of coefficients λ_i, such that the state can be written as $|\Psi_N\rangle = \sum_{i=1}^{r_\mathrm{T}} \lambda_i \bigotimes_{x=1}^{N} |v_i^x\rangle$, so $\bigotimes_{x=1}^{N} \langle v_i^x | v_j^x \rangle = \delta_{ij}$. Similar to the Schmidt rank, $r_\mathrm{T} = 1$ implies full separability of the state. It is at least NP-hard to determine the tensor rank even for pure states[147]. Moreover, the tensor rank is not additive under tensor products[148] and is known only for very few exemplary multipartite states with particular symmetries[149]. One can, however, bound the tensor rank from below by considering the Schmidt ranks with respect to all possible partitions $\alpha_i|\bar{\alpha}_i$, which we denote by r_{α_i} because it is also the rank of the corresponding reduced density matrix, $r_{\alpha_i} = \mathrm{rank}(\mathrm{Tr}_{\bar{\alpha}_i} |\Psi_N\rangle\langle\Psi_N|)$. Using this definition, it is easy to see that $r_\mathrm{T} \geq \max_i r_{\alpha_i}$. The second generalization used as an alternative to the tensor rank is the collection of the marginal ranks in the Schmidt rank vector[79] $[\vec{r}_\mathrm{S}]_i := r_{\alpha_i}$. Because there are $2^{N-1} - 1$ possible bipartitions of the system, this vector has exponentially many components, and a state is fully separable if and only if $\|\vec{r}_\mathrm{S}\|^2 = 2^{N-1} - 1$, that is, if every

Box 2 | **GME of photons**

The entanglement of more than two photons poses a unique experimental challenge — photons do not interact with each other easily, and higher-order nonlinear processes are very inefficient, rendering the direct generation of multi-photon entangled states impractical. Experiments have directly generated three-photon entanglement through cascaded down-conversion, albeit at very low count rates[207]. Multi-photon entanglement experiments have conventionally relied on the idea that two independent pairs of entangled photons are combined in such a manner as to erase their 'which-source' information[208]. This is illustrated in panel **a** of the figure, in which two photons, each from one pair of polarization-entangled photons, are combined at a polarizing beam splitter in such a manner as to erase their which-source information. A polarization-entangled Greenberger–Horne–Zeilinger (GHZ) state[209] of four photons is obtained by post-selecting on detection events at all four detectors. The first experiment based on these ideas entangled three photons in their polarization, showing the presence of a three-photon coherent superposition[210]. The same setup was later used to violate a three-particle Mermin inequality, certifying the presence of genuine multipartite entanglement (GME)[211].

Subsequent experiments have extended this idea of 'entanglement through information erasure', most recently entangling a record ten photons[212] in their polarization. Owing to the low count rates, such experiments have primarily used fidelity-based entanglement witnesses to certify GME. Parallel efforts have aimed at increasing the low probabilistic count rates achieved in multi-photon experiments by tailoring sources to reduce the degree of distinguishability of independent photons[213]. The first experiment extending multipartite entanglement (in any platform) into the high-dimensional regime was recently performed with photonic orbital angular momentum (OAM)[214] and applied the ideas of information erasure to the spatial degree of freedom through a specially designed OAM–parity beam splitter[215]. This experiment hinted at the rich structure that high-dimensional multipartite entanglement can take by creating a state entangled in $3\times3\times2$ local dimensions (Schmidt rank vector $(3, 3, 2)^T$). Even more recently, the first three-dimensional GHZ state was created with the OAM of photons[216], using the experimental setup pictured in panel **b** in the figure, in which optical elements such as beamsplitters, Dove prisms and spiral phase (OAM) holograms manipulate pairs of photons high-dimensionally entangled in their OAM to create a three-particle, three-dimensional GHZ state. Interestingly, this setup was found through the use of a computational algorithm[217,218] and used several counter-intuitive techniques departing from the symmetry of the conventional 2D techniques described above. In order to certify high-dimensional GME for these entangled states, a fidelity-based entanglement witness was used to prove that they cannot be decomposed into states of a smaller dimensionality structure[214,215].

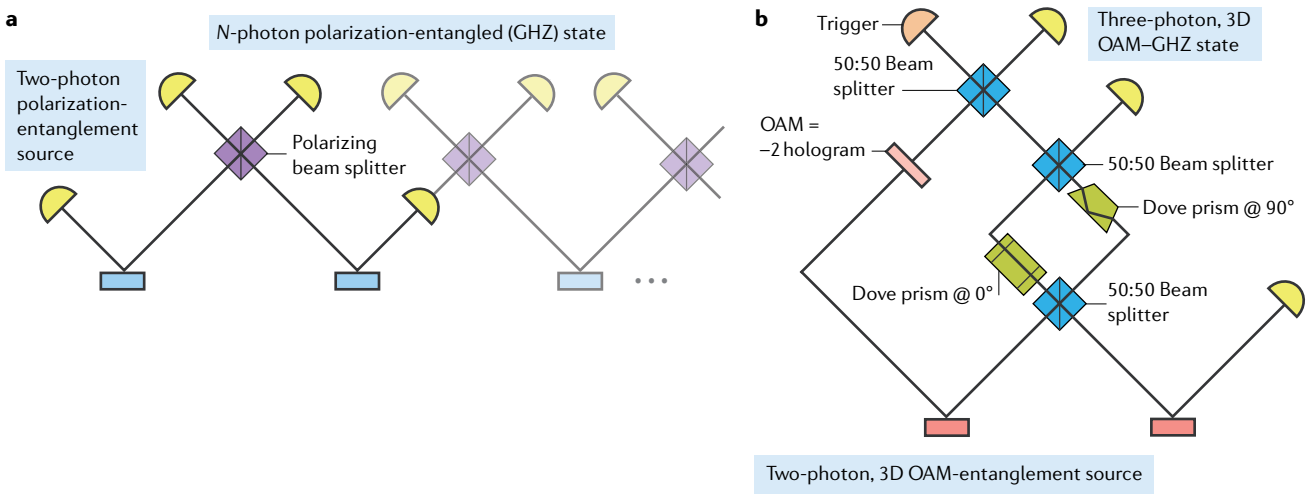

marginal rank is equal to one. Although this vector admits different ranks across different partitions, strict inequalities exist that limit the possible vectors to a non-trivial cone[150]. A consistent generalization of multipartite entanglement dimensionality can then be given as $d_{\mathrm{GME}}(\rho) := \inf_{\mathcal{D}(\rho)} \max_{|\psi_i\rangle\in\mathcal{D}(\rho)} \min_{\alpha_i} r_{\alpha_i}(|\psi_i\rangle)$.

GME classes. The tensor rank and Schmidt rank vector give further insight into multipartite entanglement structures beyond qubits, but there is still a more complex structure hidden beneath. This was first realized in REFS[151,152], proving that even genuinely multipartite states of three qubits can be inequivalent under LOCC with the famous examples of the Greenberger–Horne–Zeilinger (GHZ) state $|\mathrm{GHZ}\rangle := \frac{1}{\sqrt{2}}(|000\rangle + |111\rangle)$ and the W-state $|\mathrm{W}\rangle := \frac{1}{\sqrt{3}}(|001\rangle + |010\rangle + |100\rangle)$. This already excludes easy operational measures of entanglement that could be interpreted as asymptotic resource conversions, such as in the bipartite case. In other words, there cannot be a single universal multipartite entangled reference state from which every other state can be created by LOCC (such as the maximally entangled state for bipartite systems). Whereas infinitely many states are needed for such a source set in general[153], many cases allow finding finite maximally entangled sets of resource states to reach every other state (except for some isolated 'islands') through LOCC[154]. Another option is volume-based approaches, such as the volume of all states reachable by LOCC and the volume of all states from which a state can be reached by LOCC[155]. States for which the source volume is zero are extremal resources, whereas the target volume gives a good insight into the general utility of resource states for state transformations. Beyond deterministic transformations, one can also ask when a transformation from a state to another is possible probabilistically. This forms the basis for work in the sub-field of entanglement characterization using stochastic LOCC, which was first solved for four qubits[156] and later for all states that allow for a 'normal form', which can be filtered to local-maximally mixed states[157],

Box 3 | **GME in trapped-ion qubits**

Ion-trap platforms have been designed primarily for fault-tolerant quantum computation and simulation. The main goal is to realize a register of individually addressable qubits, in this case, trapped ions, on which arbitrary quantum gates can be applied. Although the generation of genuine multipartite entanglement (GME) is not necessarily the main application of ion-trap systems, the controlled generation and detection of GME is often considered as a means to benchmark the functionality of the devices[219]. Consequently, a first generation of ion-trap GME experiments has focused on the generation and detection of specific GME states, resulting in the observation of genuine 6-partite Greenberger–Horne–Zeilinger (GHZ)-type entanglement[220], 8-qubit W-type GME[221], with a record of 14-partite GHZ-type GME[222]. GME close to GHZ states can be detected with relatively few measurements (computational basis measurements plus parity oscillations[220,222]) using standard GME witness constructions. Nonetheless, a better characterization of the produced states and their entanglement structure can be obtained by full state tomography[223], but this approach quickly reaches its practical limits[221], because the number of measurement settings (here corresponding to global product bases with local dimension $d = 2$; TABLE 2) grows as 3^N with the number of qubits. Matrix product state tomography[224–226] can provide some relief, offering a useful pure state estimate in systems with finite interaction range, as demonstrated, for example, for 14 trapped-ion qubits[227], but this is not feasible for 20 qubits[219].

With the increasing size of the qubit registers and the desire to certify more complex (multipartite) entanglement structures (as encountered in quantum simulation[228]), it becomes necessary to identify simple witnesses based on few measurements. In REF.[219], such GME witnesses were constructed from fidelities to the closest two-qubit Bell states, averaged over all qubit pairs in groups of k neighbours within a 20-qubit chain. Intuitively, these witnesses can be understood as a form of monogamy: two-qubit entanglement between any pair in a group does not imply GME, but average two-qubit entanglement beyond certain thresholds is not compatible with an overall biseparable state. With this approach, genuine tripartite entanglement could be detected simultaneously for every triplet neighbouring qubits in a chain of 20, making use of measurements in only 3^3 (out of 3^{20}) global product bases. Using numerical search for k-body GME witnesses, the same data could be used to show the development of GME among most neighbouring quadruplets and some quintuplets.

The figure shows a simplified schematic of the (genuine multipartite) entanglement structure that develops over time under the out-of-equilibrium dynamics of an Ising-type Hamiltonian[219]. A chain of 20 initially separable qubits evolves into states with bipartite entanglement between all neighbours and, consecutively, GME between neighbouring groups of three, four and five qubits over the course of several independently measured time steps.

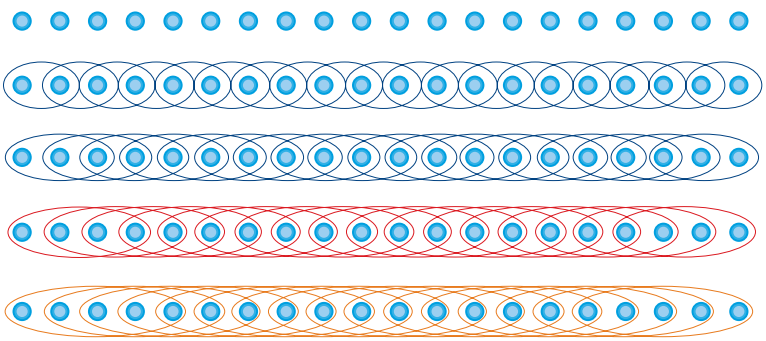

comprising all states except for a measure-zero subset. GME of photons and trapped-ion qubits is discussed in BOXES 2 and 3.

Maximal entanglement. Whereas the previous examples show that a universal notion of maximal entanglement cannot exist in the context of LOCC resource theories, one can, in principle, define states to contain the maximum amount of entanglement if they are maximally entangled across every bipartition. Such states are used in quantum error correction[134] and quantum secret sharing[158] and are called absolutely maximally entangled (AME) states. It can be shown that for every number n of parties, there is a local dimension d admitting an AME state. However, for n qubits, AME states only exist for $n = 2$, 3, 5 and 6 (REF.[159]).

Monogamy of entanglement. Another signature of entanglement in multipartite systems is the phenomenon commonly referred to as monogamy of entanglement. The name alludes to the fact that entanglement is not arbitrarily sharable among many parties. To illustrate this point, an often invoked example is that of two parties, Alice and Bob, sharing a maximally entangled state ρ_{AB} such that $E_{A:B}(\rho_{AB}) = \log_2(\min[d_A, d_B])$. This precludes any further entanglement with a third party. This example, however, is strictly true if and only if $d_A = d_B$, in which case, maximal entanglement additionally implies purity of the state ρ_{AB} and thus a tensor product structure with respect to any third party. Quantitatively, monogamy relations are often written in the form

$$E_{A:BC}(\rho_{ABC}) \leq E_{A:B}(\rho_{AB}) + E_{A:C}(\rho_{AC}) \quad (4)$$

The first prominent example valid for three qubits is the Coffman–Kundu–Wootters relation[160], in which the respective entanglement measure is the squared concurrence[45]. This was later generalized to n qubits[161] but proved not to hold for qutrits or higher dimensional systems[162]. Moreover, it has been shown that monogamy is a feature only for entanglement measures in a strict sense[163] and that monogamy and 'faithfulness' (in a geometric sense) are mutually exclusive features of entanglement measures in general dimensions[164]. Meanwhile, additive measures, such as squashed entanglement[165], are monogamous for general dimensions. The inequivalence of the two sides of the inequality (Eq. 4) can, in fact, be used to quantify and classify multipartite entanglement. For the squared concurrence of three qubits, their difference yields the three-tangle, which is non-zero only for GHZ states and can thus be used to distinguish it from biseparable or W states. A prominent property of the tangle is its invariance not only under local unitaries (SU(d)) but also under the complexification of SU(d) to SL(d) to encompass stochastic local operations. This led to the general research line of classifying multipartite entanglement in terms of stochastic LOCC using SL(d)-invariant polynomials[166,167].

PPT mixers. Analogous to the bipartite case, the convex structure of (partial) separability permits the construction of multipartite entanglement witnesses. However, the additional challenge of the potentially different partitions of density matrix decomposition elements prevents the applicability of many techniques for bipartite witnesses in multipartite systems. In particular, positive maps and their resulting witnesses are inherently connected to bipartite structures. Nonetheless, they can be harnessed as constraints for positive semi-definite programming. This follows from the simple observation that a state that is decomposable into bi-product states is, for instance, also decomposable into PPT states. This insight has led to the concept of PPT mixers[168], yielding effective numerical tools for low dimensions. At the

Box 4 | **Cold-atom entanglement**

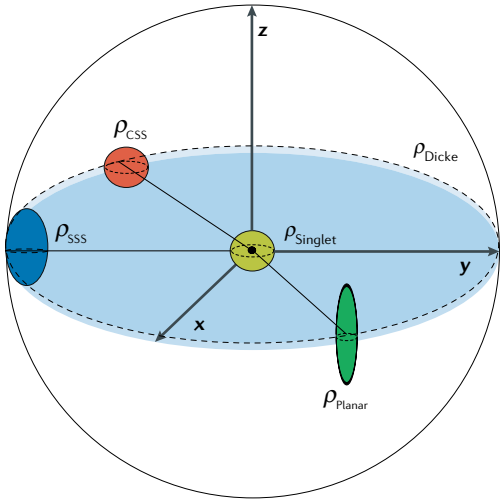

Experimentally, entanglement through spin squeezing has been demonstrated extensively in atomic ensembles[142,146]. There are two underlying mechanisms: atom–atom interactions in Bose–Einstein condensates and light–atom interactions in ensembles of atoms at room temperature or cold atomic ensembles. In such systems, state tomography is usually performed on a collective Bloch sphere of three orthogonal collective spin directions. The mean spin polarization $\langle \vec{J} \rangle = (\langle J_x \rangle, \langle J_y \rangle, J_z \rangle)$ can be depicted as a vector, together with variances $(\Delta J_k)^2$ as uncertainty regions around it[142,146]. Other collective $su(2j+1)$ operators and thus correspondingly different collective Bloch spheres have also been recently considered in spinor ensembles[229,230].

An example of dynamics that produce spin squeezing through atom–atom interactions is the one-axis twisting dynamics, $H_{OT} \propto J_x^2$, employed in several experiments with Bose–Einstein condensates[231–237]. For the second group, a widely used method is the production of spin squeezing through quantum non-demolition measurement and feedback, which consists of sending pulses of light through the ensemble of atoms and engineering the interaction $H_{QND} \propto S_z J_z$, which rotates the light polarization and conserves J_z. This technique has been used in both cold and room-temperature atomic ensembles[238–241], as well as with an additional coupling to an optical cavity, which enhances the optical depth of the ensemble[242–246]. Notably, entanglement (with a depth of up to a few thousands) has also been achieved through other regimes of light-mediated atomic interactions[247–250], and quantum non-demolition measurements have been used to entangle two macroscopic room-temperature vapour cells[251].

Recently, generalized spin-squeezed states, such as singlet states[252] or planar squeezed states[75,253], have been investigated in experiments with atomic ensembles and have been proposed for application in quantum metrology. In particular, Dicke states are attracting increasing attention and are produced in experiments with Bose–Einstein condensates[188,229,254], with atomic spin-mixing dynamics resembling parametric down-conversion of photons to some extent. A depth of entanglement of several hundreds has been inferred with collective measurements for these generalized spin-squeezed states[75,188,255–257]. Finally, current experimental efforts have been oriented towards demonstrating entanglement between spatially separated parts of Bose–Einstein condensates (still in localized traps)[67,230,258].

The illustration shows generalized spin-squeezed states in the collective Bloch sphere. States are represented as vectors (for the global spin length $\langle \vec{J} \rangle$) with uncertainty regions around them. These regions also take into account classical (usually Poissonian) noise. ρ_{CSS} is a completely polarized, mixed state $|\langle \vec{J} \rangle| \simeq O(N)$ close to a coherent spin state that has three variances of the order of $(\Delta J_k) \simeq O(\sqrt{N})$; ρ_{SSS} is completely polarized and has a single squeezed variance in a direction orthogonal to its polarization; ρ_{Planar} is a planar squeezed state and is almost completely polarized with two squeezed variances; $\rho_{Singlet}$ is a macroscopic singlet state, with all three variances squeezed; ρ_{Dicke} is the unpolarized Dicke state, with a tiny uncertainty $(\Delta J_z) \approx 0$ and large $(\Delta J_x) = (\Delta J_y) \approx O(N)$.

same time, this connection can be used to effectively lift bipartite witnesses for multipartite usage[169,170] and to obtain generalizations to maps that are positive on biseparable states[171].

GME witnesses. A canonical form of GME witnesses can be obtained by harnessing the different Schmidt decompositions across bipartitions. For instance, for a pure target state $|\psi_T\rangle$, computing all marginal eigenvalues allows defining a witness[172] of the form $W_{GME} := \max_{\alpha_i} \|\rho_{\alpha_i}\|_\infty \mathbb{1} - |\psi_T\rangle\langle\psi_T|$. Apart from this generically applicable method, most available GME witnesses are tailored towards detecting specific multipartite entangled states, such as graph states[173] or stabilizer states[139,140], Dicke states[174] or generally symmetric states[175].

Leaving the regime of linear operators and moving on to nonlinear functions of density matrix elements, more powerful certification techniques exist. In REFS[176,177], nonlinear inequalities for detecting multipartite entanglement in GHZ and W-like states were introduced, which were proved to be strictly more powerful than the canonical form introduced above. Moreover, these nonlinear inequalities were later shown to provide lower bounds on a particular measure of genuine multipartite entanglement, the GME-concurrence[77]. In fact, one can leverage positive semi-definite programming techniques to numerically evaluate multiple suitable convex-roof-based entanglement measures[178]. In a separate approach, separability eigenvalues were introduced as a means to construct multipartite entanglement witnesses[179].

Entanglement and spin squeezing. A well-understood many-body system is an ensemble of N (pseudo)spins manipulated (and measured) collectively in a trap (BOX 4). To detect entanglement, spin-squeezing criteria for entanglement have been derived. These are based on an analogy with bosonic quadratures and are connected with uncertainty relations of collective spin components. A necessary condition for all fully separable states of N particles with spin-1/2 reads

$$\xi_S^2 := N \frac{(\Delta J_z)^2}{\langle J_x \rangle^2 + |J_y\rangle^2} \geq 1,$$

which also directly connects entanglement with enhanced sensitivity in Ramsey spectroscopy with totally polarized ensembles of atoms[73,180–182]. Here, $(\Delta J_z)^2$ is the smallest variance in a direction orthogonal to the polarization, such as $|\langle J_y \rangle| \approx N/2$, and a spin-squeezed state is obtained when $\xi_S^2 < 1$, where the boundary value defines the coherent spin states.

As a generalization, a full set of spin-squeezing inequalities, which have the geometrical shape of a closed convex polytope and define a more general spin-squeezing quantifier, has been derived for spin-1/2 ensembles[183,184] and later generalized to all higher spin-j ensembles and to $su(d)$ observables different from angular momentum components[185,186]. Thus, witnessing entanglement through the squeezing of the collective spin of an ensemble is convenient because this notion is captured by a simple polytope in the space of collective spin variances. A similar simple structure remains even for device-independent certification of entanglement based on collective measurements[187].

Entanglement depth is typically used as a quantifier of entanglement in spin-squeezed states, which can also be witnessed with spin-squeezing parameters by making use of the Legendre transform method[73–75]. The general picture is that one can find a hierarchy of bounds on some collective quantities that depend on the entanglement depth, such as $(\Delta J_z)^2 \geq N j F_j(\frac{\langle J_y \rangle}{Nj})$, where F_j is a certain convex function that can be obtained through

Legendre transforms. A state with the property that the variance on the left-hand side is smaller than the quantity on the right-hand side for a certain F_j is detected with a depth of entanglement of at least $k = J/j$, where j is the spin quantum number of the individual particles. Similar entanglement depth criteria have also been derived for different target states, like Dicke states[74,188] and planar quantum squeezed states[75,189], as well as based on other quantities, such as the quantum Fisher information[133,190–192].

Entanglement in optical lattices. A current challenge is to demonstrate and exploit multipartite entanglement in spatially extended systems, such as optical lattices. Here, as for localized traps, the most common measurement consists of releasing the gas from the trap (the lattice potential) and imaging the expanding gas, inferring the momentum distribution of the original system of particles. Besides spin-squeezing methods that could also be used in these systems, criteria to detect entanglement in optical lattices have been proposed based on quantities obtained from density measurements after a certain time of flight[193,194]. Furthermore, some collective quantities with thermodynamical significance, such as energy[195,196] or susceptibilities[197–199] (for instance, to external magnetic fields), could be used for entanglement detection in such extended systems. These quantities can be extracted from the structure factors coming from neutron scattering cross sections[76,194,198,200,201]. Some of these methods have been used for a first experimental demonstration (and quantification) of entanglement in a bosonic optical lattice[200], whereas other recent experiments[202–204] demonstrated entanglement between two spins in a lattice or a superlattice.

Outlook

Entanglement certification cannot be exhaustively covered in a single review. For the sake of brevity, we mainly discussed the case of well-characterized measurement devices and system Hamiltonians. It is indeed possible to transcend this paradigm and obtain robust entanglement certification techniques that do not require a detailed physical understanding of the measurement procedure or the investigated system. These device-independent certification techniques currently require more resources and suffer from poor robustness to experimental noise. As quantum technologies evolve, the logical next step is to move towards more device-independent certification techniques, increasing the security in quantum communication and the trust in the correct functionality of quantum devices.

Finally, whereas the use of bipartite high-dimensional entanglement is well established, the unfathomable complexity of multipartite quantum correlations has so far only found few applications in many-party protocols, and for some applications, they may not be useful at all (for example, universal quantum computation[205]). Finding further compelling quantum information protocols would motivate a deeper investigation of the structure of multipartite entanglement and guide theoretical and experimental efforts towards the preparation, manipulation and certification of novel many-body quantum states.

Published online 19 December 2018

1. Einstein, A., Podolsky, B. & Rosen, N. Can quantum-mechanical description of physical reality be considered complete? *Phys. Rev.* **47**, 777–780 (1935).
2. Bell, J. S. On the Einstein Podolsky Rosen Paradox. *Physics* **1**, 195–200 (1964).
3. Bouwmeester, D. et al. Experimental Quantum Teleportation. *Nature* **390**, 575–579 (1997).
4. Weihs, G., Jennewein, T., Simon, C., Weinfurter, H. & Zeilinger, A. Violation of Bell's Inequality under Strict Einstein Locality Conditions. *Phys. Rev. Lett.* **81**, 5039–5043 (1998).
5. Poppe, A. et al. Practical Quantum Key Distribution with Polarization-Entangled Photons. *Opt. Express* **12**, 3865–3871 (2004).
6. Ursin, R. et al. Entanglement-based quantum communication over 144 km. *Nat. Phys.* **3**, 481–486 (2007).
7. Brunner, N., Cavalcanti, D., Pironio, S., Scarani, V. & Wehner, S. Bell nonlocality. *Rev. Mod. Phys.* **86**, 419–478 (2014).
8. Hensen, B. et al. Loophole-free Bell inequality violation using electron spins separated by 1.3 kilometres. *Nature* **526**, 682–686 (2015).
9. Giustina, M. et al. Significant-Loophole-Free Test of Bell's Theorem with Entangled Photons. *Phys. Rev. Lett.* **115**, 250401 (2015).
10. Shalm, L. K. et al. Strong Loophole-Free Test of Local Realism. *Phys. Rev. Lett.* **115**, 250402 (2015).
11. Werner, R. F. Quantum states with Einstein-Podolsky-Rosen correlations admitting a hidden-variable model. *Phys. Rev. A* **40**, 4277 (1989).
12. Barrett, J. Nonsequential positive-operator-valued measurements on entangled mixed states do not always violate a Bell inequality. *Phys. Rev. A* **65**, 042302 (2002).
13. Acín, A., Gisin, N. & Toner, B. Grothendieck's constant and local models for noisy entangled quantum states. *Phys. Rev. A* **73**, 062105 (2006).
14. Vértesi, T. More efficient Bell inequalities for Werner states. *Phys. Rev. A* **78**, 032112 (2008).
15. Hirsch, F., Quintino, M. T., Vértesi, T., Navascués, M. & Brunner, N. Better local hidden variable models for two-qubit Werner states and an upper bound on the Grothendieck constant $K_G(3)$. *Quantum* **1**, 3 (2017).
16. Bruß, D. Characterizing Entanglement. *J. Math. Phys.* **43**, 4237–4251 (2002).
17. Plenio, M. B. & Virmani, S. An introduction to entanglement measures. *Quant. Inf. Comput.* **7**, 1 (2007).
18. Eltschka, C. & Siewert, J. Quantifying entanglement resources. *J. Phys. A: Math. Theor.* **47**, 424005 (2014).
19. Horodecki, R., Horodecki, P., Horodecki, M. & Horodecki, K. Quantum entanglement. *Rev. Mod. Phys.* **81**, 865–942 (2009).
20. Gühne, O. & Tóth, G. Entanglement detection. *Phys. Rep.* **474**, 1–75 (2009).
21. Cerf, N. J., Bourennane, M., Karlsson, A. & Gisin, N. Security of Quantum Key Distribution Using *d*-Level Systems. *Phys. Rev. Lett.* **88**, 127902 (2002).
22. Barrett, J., Kent, A. & Pironio, S. Maximally Nonlocal and Monogamous Quantum Correlations. *Phys. Rev. Lett.* **97**, 170409 (2006).
23. Gröblacher, S., Jennewein, T., Vaziri, A., Weihs, G. & Zeilinger, A. Experimental quantum cryptography with qutrits. *New J. Phys.* **8**, 75 (2006).
24. Huber, M. & Pawlowski, M. Weak randomness in device independent quantum key distribution and the advantage of using high dimensional entanglement. *Phys. Rev. A* **88**, 032309 (2013).
25. Jozsa, R. & Linden, N. On the Role of Entanglement in Quantum-Computational Speed-Up. *Proc. Roy. Soc. A Math. Phys.* **459**, 2011–2032 (2003).
26. Amico, L., Fazio, R., Osterloh, A. & Vedral, V. Entanglement in many-body systems. *Rev. Mod. Phys.* **80**, 517–576 (2008).
27. Verstraete, F., Murg, V. & Cirac, J. I. Matrix product states, projected entangled pair states, and variational renormalization group methods for quantum spin systems. *Adv. Phys.* **57**, 143–224 (2008).
28. Eisert, J., Cramer, M. & Plenio, M. B. Colloquium: Area laws for the entanglement entropy. *Rev. Mod. Phys.* **82**, 277–306 (2010).
29. Wineland, D. J., Bollinger, J. J., Itano, W. M., Moore, F. L. & Heinzen, D. J. Spin squeezing and reduced quantum noise in spectroscopy. *Phys. Rev. A* **46**, R6797 (1992).
30. Huelga, S. F. et al. On the Improvement of Frequency Stardards with Quantum Entanglement. *Phys. Rev. Lett.* **79**, 3865 (1997).
31. Giovannetti, V., Lloyd, S. & Maccone, L. Quantum Metrology. *Phys. Rev. Lett.* **96**, 010401 (2006).
32. Maccone, L. Intuitive reason for the usefulness of entanglement in quantum metrology. *Phys. Rev. A* **88**, 042109 (2013).
33. Friis, N. et al. Flexible resources for quantum metrology. *New J. Phys.* **19**, 063044 (2017).
34. Tóth, G. & Apellaniz, I. Quantum metrology from a quantum information science perspective. *J. Phys. A: Math. Theor.* **47**, 424006 (2014).
35. Acín, A. et al. The quantum technologies roadmap: a European community view. *New J. Phys.* **20**, 080201 (2018).
36. Andersen, U. L., Leuchs, G. & Silberhorn, C. Continuous-variable quantum information processing. *Laser Photonics Rev.* **4**, 337–354 (2010).
37. Weedbrook, C. et al. Gaussian quantum information. *Rev. Mod. Phys.* **84**, 621–669 (2012).
38. Adesso, G., Ragy, S. & Lee, A. R. Continuous Variable Quantum Information: Gaussian States and Beyond. *Open Syst. Inf. Dyn.* **21**, 1440001 (2014).
39. Nielsen, M. A. Conditions for a Class of Entanglement Transformations. *Phys. Rev. Lett.* **83**, 436 (1999).
40. Chitambar, E., Leung, D., Mančinska, L., Ozols, M. & Winter, A. Everything You Always Wanted to Know About LOCC (But Were Afraid to Ask). *Commun. Math. Phys.* **328**, 303–326 (2014).
41. Gurvits, L. Classical complexity and quantum entanglement. *J. Comput. Syst. Sci.* **69**, 448–484 (2004).
42. Gharibian, S. Strong NP-hardness of the quantum separability problem. *Quantum Inf. Comput.* **10**, 343–360 (2010).

43. Nielsen, M. A. & Vidal, G. Majorization and the interconversion of bipartite states. *Quant. Inf. Comput.* **1**, 76–93 (2001).
44. Bennett, C. H., Di Vincenzo, D. P., Smolin, J. A. & Wootters, W. K. Mixed-state entanglement and quantum error correction. *Phys. Rev. A* **54**, 3824 (1996).
45. Wootters, W. K. Entanglement of Formation of an Arbitrary State of Two Qubits. *Phys. Rev. Lett.* **80**, 2245 (1998).
46. Hayden, P. M., Horodecki, M. & Terhal, B. M. The asymptotic entanglement cost of preparing a quantum state. *J. Phys. A: Math. Gen.* **34**, 6891–6898 (2001).
47. Bennett, C. H., Bernstein, H. J., Popescu, S. & Schumacher, B. Concentrating Partial Entanglement by Local Operations. *Phys. Rev. A* **53**, 2046–2052 (1996).
48. Bennett, C. H. et al. Purification of Noisy Entanglement and Faithful Teleportation via Noisy Channels. *Phys. Rev. Lett.* **76**, 722–725 (1996).
49. Hastings, M. B. A Counterexample to Additivity of Minimum Output Entropy. *Nat. Phys.* **5**, 255–257 (2009).
50. Terhal, B. M. & Horodecki, P. Schmidt number for density matrices. *Phys. Rev. A* **61**, 040301 (2000).
51. Altepeter, J. B., James, D. F. V. & Kwiat, P. G. in *Quantum State Estimation* (eds Paris, M. & Řeháček) 113–145 (Springer, Berlin, Heidelberg, 2004).
52. Ansmann, M. et al. Measurement of the entanglement of two superconducting qubits via state tomography. *Science* **313**, 1423 (2006).
53. Peres, A. Separability Criterion for Density Matrices. *Phys. Rev. Lett.* **77**, 1413 (1996).
54. Horodecki, M., Horodecki, P. & Horodecki, R. Separability of mixed states: necessary and sufficient conditions. *Phys. Lett. A* **223**, 25 (1996).
55. Horodecki, M., Horodecki, P. & Horodecki, R. Mixed-State Entanglement and Distillation: Is there a "Bound" Entanglement in Nature? *Phys. Rev. Lett.* **80**, 5239 (1998).
56. Pankowski, Ł., Piani, M., Horodecki, M. & Horodecki, P. A Few Steps More Towards NPT Bound Entanglement. *IEEE Trans. Inf. Theory* **56**, 4085–4100 (2010).
57. Watrous, J. Many Copies May Be Required for Entanglement Distillation. *Phys. Rev. Lett.* **93**, 010502 (2004).
58. Plenio, M. B. Logarithmic Negativity: A Full Entanglement Monotone That is not Convex. *Phys. Rev. Lett.* **95**, 090503 (2005).
59. Vidal, G. Entanglement monotones. *J. Mod. Opt.* **47**, 355–376 (2000).
60. Eisert, J. *Entanglement in quantum information theory*. Thesis, Univ. Potsdam (2001).
61. Vidal, G. & Werner, R. F. Computable measure of entanglement. *Phys. Rev. A* **65**, 032314 (2002).
62. Hofmann, H. F. & Takeuchi, S. Violation of local uncertainty relations as a signature of entanglement. *Phys. Rev. A* **68**, 032103 (2003).
63. Gühne, O., Mechler, M., Tóth, G. & Adam, P. Entanglement criteria based on local uncertainty relations are strictly stronger than the computable cross norm criterion. *Phys. Rev. A* **74**, 010301 (2006).
64. Zhang, C.-J., Nha, H., Zhang, Y.-S. & Guo, G.-C. Entanglement detection via tighter local uncertainty relations. *Phys. Rev. A* **81**, 012324 (2010).
65. Schwonnek, R., Dammeier, L. & Werner, R. F. State-Independent Uncertainty Relations and Entanglement Detection in Noisy Systems. *Phys. Rev. Lett.* **119**, 170404 (2017).
66. Reid, M. D. Demonstration of the Einstein-Podolsky-Rosen paradox using nondegenerate parametric amplification. *Phys. Rev. A* **40**, 913–923 (1989).
67. Lange, K. et al. Entanglement between two spatially separated atomic modes. *Science* **360**, 416–418 (2018).
68. Reid, M. D. et al. Colloquium: The Einstein-Podolsky-Rosen paradox: From concepts to applications. *Rev. Mod. Phys.* **81**, 1727–1751 (2009).
69. Gühne, O., Hyllus, P., Gittsovich, O. & Eisert, J. Covariance Matrices and the Separability Problem. *Phys. Rev. Lett.* **99**, 130504 (2007).
70. Gittsovich, O., Gühne, O., Hyllus, P. & Eisert, J. Unifying several separability conditions using the covariance matrix criterion. *Phys. Rev. A* **78**, 052319 (2008).
71. Gühne, O., Reimpell, M. & Werner, R. F. Estimating Entanglement Measures in Experiments. *Phys. Rev. Lett.* **98**, 110502 (2007).
72. Eisert, J., Brandão, F. G. S. L. & Audenaert, K. M. R. Quantitative entanglement witnesses. *New J. Phys.* **9**, 46 (2007).
73. Sørensen, A. & Mølmer, K. Entanglement and Extreme Spin Squeezing. *Phys. Rev. Lett.* **86**, 4431–4434 (2001).
74. Vitagliano, G. et al. Entanglement and extreme spin squeezing of unpolarized states. *New J. Phys.* **19**, 013027 (2017).
75. Vitagliano, G. et al. Entanglement and extreme planar spin squeezing. *Phys. Rev. A* **97**, 020301 (2018).
76. Marty, O., Cramer, M., Vitagliano, G., Tóth, G. & Plenio, M. B. Multiparticle entanglement criteria for nonsymmetric collective variances. Preprint at https://arxiv.org/abs/1708.06986 (2017).
77. Ma, Z.-H. et al. Measure of genuine multipartite entanglement with computable lower bounds. *Phys. Rev. A* **83**, 062325 (2011).
78. Wu, J.-Y., Kampermann, H., Bruß, D., Klöckl, C. & Huber, M. Determining lower bounds on a measure of multipartite entanglement from few local observables. *Phys. Rev. A* **86**, 022319 (2012).
79. Huber, M. & de Vicente, J. I. Structure of Multidimensional Entanglement in Multipartite Systems. *Phys. Rev. Lett.* **110**, 030501 (2013).
80. Bertlmann, R. A. & Krammer, P. Bloch vectors for qudits. *J. Phys. A: Math. Theor.* **41**, 235303 (2008).
81. Bavaresco, J. et al. Measurements in two bases are sufficient for certifying high-dimensional entanglement. *Nat. Phys.* **14**, 1032–1037 (2018).
82. Blume-Kohout, R., Yin, J. O. S. & van Enk, S. J. Entanglement Verification with Finite Data. *Phys. Rev. Lett.* **105**, 170501 (2010).
83. Flammia, S. T. & Liu, Y.-K. Direct Fidelity Estimation from Few Pauli Measurements. *Phys. Rev. Lett.* **106**, 230501 (2011).
84. Aolita, L., Gogolin, C., Kliesch, M. & Eisert, J. Reliable quantum certification for photonic quantum technologies. *Nat. Commun.* **6**, 8498 (2015).
85. Schwemmer, C. et al. Systematic Errors in Current Quantum State Tomography Tools. *Phys. Rev. Lett.* **114**, 080403 (2015).
86. Ferrie, C. & Blume-Kohout, R. Maximum likelihood quantum state tomography is inadmissible. Preprint at https://arxiv.org/abs/1808.01072 (2018).
87. Pallister, S., Linden, N. & Montanaro, A. Optimal Verification of Entangled States with Local Measurements. *Phys. Rev. Lett.* **120**, 170502 (2018).
88. Tiranov, A. et al. Quantification of multidimensional entanglement stored in a crystal. *Phys. Rev. A* **96**, 040303 (2017).
89. Martin, A. et al. Quantifying Photonic High-Dimensional Entanglement. *Phys. Rev. Lett.* **118**, 110501 (2017).
90. Steinlechner, F. et al. Distribution of high-dimensional entanglement via an intra-city free-space link. *Nat. Commun.* **8**, 15971 (2017).
91. Schneeloch, J. & Howland, G. A. Quantifying high-dimensional entanglement with Einstein-Podolsky-Rosen correlations. *Phys. Rev. A* **97**, 042338 (2018).
92. Erker, P., Krenn, M. & Huber, M. Quantifying high dimensional entanglement with two mutually unbiased bases. *Quantum* **1**, 22 (2017).
93. Tasca, D. S., Sánchez, P. & Walborn, S. P. & Rudnicki, Ł. Mutual Unbiasedness in Coarse-Grained Continuous Variables. *Phys. Rev. Lett.* **120**, 040403 (2018).
94. Piani, M. & Mora, C. E. Class of positive-partial-transpose bound entangled states associated with almost any set of pure entangled states. *Phys. Rev. A* **75**, 012305 (2007).
95. Gour, G. Family of concurrence monotones and its applications. *Phys. Rev. A* **71**, 012318 (2005).
96. Sentís, G., Eltschka, C., Gühne, O., Huber, M. & Siewert, J. Quantifying Entanglement of Maximal Dimension in Bipartite Mixed States. *Phys. Rev. Lett.* **117**, 190502 (2016).
97. Kraft, T., Ritz, C., Brunner, N., Huber, M. & Gühne, O. Characterizing Genuine Multilevel Entanglement. *Phys. Rev. Lett.* **120**, 060502 (2018).
98. Guo, Y. et al. Experimental witness of genuine high-dimensional entanglement. *Phys. Rev. A* **97**, 062309 (2018).
99. Szarek, S. J., Werner, E. & Życzkowski, K. How often is a random quantum state *k*-entangled? *J. Phys. A: Math. Theor.* **44**, 045303 (2011).
100. Huber, M., Lami, L., Lancien, C. & Müller-Hermes, A. High-Dimensional Entanglement in states with positive partial transposition. *Phys. Rev. Lett.* **121**, 200503 (2018).
101. Sanpera, A., Bruß, D. & Lewenstein, M. Schmidt-number witnesses and bound entanglement. *Phys. Rev. A* **63**, 050301 (2001).
102. Miatto, F. M. et al. Bounds and optimisation of orbital angular momentum bandwidths within parametric down-conversion systems. *Eur. Phys. J. D.* **66**, 178 (2012).
103. Allen, L., Beijersbergen, M., Spreeuw, R. J. C. & Woerdman, J. P. Orbital angular momentum of light and the transformation of Laguerre-Gaussian laser modes. *Phys. Rev. A* **45**, 8185–8189 (1992).
104. Krenn, M., Malik, M., Erhard, M. & Zeilinger, A. Orbital angular momentum of photons and the entanglement of Laguerre-Gaussian modes. *Philos. Trans. R. Soc. A* **375**, 20150442 (2017).
105. Collins, D., Gisin, N., Linden, N., Massar, S. & Popescu, S. Bell Inequalities for Arbitrarily High-Dimensional Systems. *Phys. Rev. Lett.* **88**, 040404 (2002).
106. Vaziri, A., Weihs, G. & Zeilinger, A. Experimental Two-Photon, Three-Dimensional Entanglement for Quantum Communication. *Phys. Rev. Lett.* **89**, 240401 (2002).
107. Krenn, M. et al. Generation and confirmation of a (100×100)-dimensional entangled quantum system. *Proc. Natl. Acad. Sci. U. S. A.* **111**, 6243–6247 (2014).
108. Dada, A. C., Leach, J., Buller, G. S., Padgett, M. J. & Andersson, E. Experimental high-dimensional two-photon entanglement and violations of generalized Bell inequalities. *Nat. Phys.* **7**, 677–680 (2011).
109. O'Sullivan, M., Ali Khan, I., Boyd, R. W. & Howell, J. Pixel Entanglement: Experimental Realization of Optically Entangled d = 3 and d = 6 Qudits. *Phys. Rev. Lett.* **94**, 220501 (2005).
110. Edgar, M. P. et al. Imaging high-dimensional spatial entanglement with a camera. *Nat. Commun.* **3**, 984 (2012).
111. Moreau, P.-A., Devaux, F. & Lantz, E. Einstein-Podolsky-Rosen Paradox in Twin Images. *Phys. Rev. Lett.* **113**, 160401 (2014).
112. Howland, G. A., Knarr, S. H., Schneeloch, J., Lum, D. J. & Howell, J. C. Compressively Characterizing High-Dimensional Entangled States with Complementary, Random Filtering. *Phys. Rev. X* **6**, 021018 (2016).
113. Tasca, D. S. et al. Testing for entanglement with periodic coarse graining. *Phys. Rev. A* **97**, 042312 (2018).
114. Law, C. K. & Eberly, J. H. Analysis and Interpretation of High Transverse Entanglement in Optical Parametric Down Conversion. *Phys. Rev. Lett.* **92**, 127903 (2004).
115. Matthews, J. C. F., Politi, A., Stefanov, A. & O'Brien, J. L. Manipulation of multiphoton entanglement in waveguide quantum circuits. *Nat. Photonics* **3**, 346–350 (2009).
116. Sansoni, L. et al. Polarization Entangled State Measurement on a Chip. *Phys. Rev. Lett.* **105**, 200503 (2010).
117. Schaeff, C., Polster, R., Huber, M., Ramelow, S. & Zeilinger, A. Experimental access to higher-dimensional entangled quantum systems using integrated optics. *Optica* **2**, 523–529 (2015).
118. Salavrakos, A. et al. Bell Inequalities Tailored to Maximally Entangled States. *Phys. Rev. Lett.* **119**, 040402 (2017).
119. Wang, J. et al. Multidimensional quantum entanglement with large-scale integrated optics. *Science* **360**, 285–291 (2018).
120. de Riedmatten, H., Marcikic, I., Zbinden, H. & Gisin, N. Creating high dimensional time-bin entanglement using mode-locked lasers. *Quantum Inf. Comput.* **2**, 425–433 (2002).
121. Thew, R. T., Acín, A., Zbinden, H. & Gisin, N. Bell-Type Test of Energy-Time Entangled Qutrits. *Phys. Rev. Lett.* **93**, 010503 (2004).
122. Bessire, B., Bernhard, C., Feurer, T. & Stefanov, A. Versatile shaper-assisted discretization of energy–time entangled photons. *New J. Phys.* **16**, 033017 (2014).
123. Kues, M. et al. On-chip generation of high-dimensional entangled quantum states and their coherent control. *Nature* **546**, 622–626 (2017).
124. Barreiro, J., Langford, N., Peters, N. & Kwiat, P. Generation of Hyperentangled Photon Pairs. *Phys. Rev. Lett.* **95**, 260501 (2005).
125. Anderson, B. E., Sosa-Martinez, H., Riofrío, C. A., Deutsch, I. H. & Jessen, P. S. Accurate and Robust Unitary Transformations of a High-Dimensional Quantum System. *Phys. Rev. Lett.* **114**, 240401 (2015).

126. Kumar, K. S., Vepsäläinen, A., Danilin, S. & Paraoanu, G. S. Stimulated Raman adiabatic passage in a three-level superconducting circuit. *Nat. Commun.* **7**, 10628 (2016).
127. Wang, Y. et al. Quantum Simulation of Helium Hydride Cation in a Solid-State Spin Register. *ACS Nano* **9**, 7769–7774 (2015).
128. Riedinger, R. et al. Remote quantum entanglement between two micromechanical oscillators. *Nature* **556**, 473–477 (2018).
129. Epping, M., Kampermann, H., Macchiavello, C. & Bruß, D. Multi-partite entanglement can speed up quantum key distribution in networks. *New J. Phys.* **19**, 093012 (2017).
130. Pivoluska, M., Huber, M. & Malik, M. Layered quantum key distribution. *Phys. Rev. A* **97**, 032312 (2018).
131. Ribeiro, J., Murta, G. & Wehner, S. Fully device-independent conference key agreement. *Phys. Rev. A* **97**, 022307 (2018).
132. Bäuml, S. & Azuma, K. Fundamental limitation on quantum broadcast networks. *Quantum Sci. Technol.* **2**, 024004 (2017).
133. Tóth, G. Multipartite entanglement and high-precision metrology. *Phys. Rev. A* **85**, 022322 (2012).
134. Scott, A. J. Multipartite entanglement, quantum-error-correcting codes, and entangling power of quantum evolutions. *Phys. Rev. A* **69**, 052330 (2004).
135. Bruß, D. & Macchiavello, C. Multipartite entanglement in quantum algorithms. *Phys. Rev. A* **83**, 052313 (2011).
136. Raussendorf, R. & Briegel, H. J. A One-Way Quantum Computer. *Phys. Rev. Lett.* **86**, 5188–5191 (2001).
137. Hein, M., Eisert, J. & Briegel, H. J. Multiparty entanglement in graph states. *Phys. Rev. A* **69**, 062311 (2004).
138. Rossi, M., Huber, M., Bruß, D. & Macchiavello, C. Quantum hypergraph states. *New J. Phys.* **15**, 113022 (2013).
139. Tóth, G. & Gühne, O. Entanglement detection in the stabilizer formalism. *Phys. Rev. A* **72**, 022340 (2005).
140. Audenaert, K. M. R. & Plenio, M. B. Entanglement on mixed stabilizer states: normal forms and reduction procedures. *New J. Phys.* **7**, 170 (2005).
141. Gogolin, C. & Eisert, J. Equilibration, thermalisation, and the emergence of statistical mechanics in closed quantum systems. *Rep. Prog. Phys.* **79**, 056001 (2016).
142. Ma, J., Wang, X., Sun, C. P. & Nori, F. Quantum spin squeezing. *Phys. Rep.* **509**, 89–165 (2011).
143. Kelly, J. et al. State preservation by repetitive error detection in a superconducting quantum circuit. *Nature* **519**, 66–69 (2015).
144. Song, C. et al. 10-Qubit Entanglement and Parallel Logic Operations with a Superconducting Circuit. *Phys. Rev. Lett.* **119**, 180511 (2017).
145. Gühne, O., Tóth, G. & Briegel, H. J. Multipartite entanglement in spin chains. *New J. Phys.* **7**, 229 (2005).
146. Pezzè, L., Smerzi, A., Oberthaler, M. K., Schmied, R. & Treutlein, P. Quantum metrology with nonclassical states of atomic ensembles. *Rev. Mod. Phys.* **90**, 035005 (2018).
147. Håstad, J. Tensor rank is NP-complete. *J. Algorithm* **11**, 644–654 (1990).
148. Christandl, M., Jensen, A. K. & Zuiddam, J. Tensor rank is not multiplicative under the tensor product. *Lin. Alg. Appl.* **543**, 125–139 (2018).
149. Chen, L., Chitambar, E., Duan, R., Ji, Z. & Winter, A. Tensor Rank and Stochastic Entanglement Catalysis for Multipartite Pure States. *Phys. Rev. Lett.* **105**, 200501 (2010).
150. Cadney, J., Huber, M., Linden, N. & Winter, A. Inequalities for the ranks of multipartite quantum states. *Lin. Alg. Appl.* **452**, 153–171 (2014).
151. Dür, W., Vidal, G. & Cirac, J. I. Three qubits can be entangled in two inequivalent ways. *Phys. Rev. A* **62**, 062314 (2000).
152. Acín, A., Bruß, D., Lewenstein, M. & Sanpera, A. Classification of Mixed Three-Qubit States. *Phys. Rev. Lett.* **87**, 040401 (2001).
153. Gour, G., Kraus, B. & Wallach, N. R. Almost all multipartite qubit quantum states have trivial stabilizer. *J. Math. Phys.* **58**, 092204 (2017).
154. de Vicente, J. I., Spee, C. & Kraus, B. Maximally Entangled Set of Multipartite Quantum States. *Phys. Rev. Lett.* **111**, 110502 (2013).
155. Schwaiger, K., Sauerwein, D., Cuquet, M., de Vicente, J. I. & Kraus, B. Operational Multipartite Entanglement Measures. *Phys. Rev. Lett.* **115**, 150502 (2015).
156. Verstraete, F., Dehaene, J., De Moor, B. & Verschelde, H. Four qubits can be entangled in nine different ways. *Phys. Rev. A* **65**, 052112 (2002).
157. Verstraete, F., Dehaene, J. & De Moor, B. Normal forms and entanglement measures for multipartite quantum states. *Phys. Rev. A* **68**, 012103 (2003).
158. Helwig, W., Cui, W., Latorre, J. I., Riera, A. & Lo, H.-K. Absolute maximal entanglement and quantum secret sharing. *Phys. Rev. A* **86**, 052335 (2012).
159. Huber, F., Gühne, O. & Siewert, J. Absolutely Maximally Entangled States of Seven Qubits Do Not Exist. *Phys. Rev. Lett.* **118**, 200502 (2017).
160. Coffman, V., Kundu, J. & Wootters, W. K. Distributed entanglement. *Phys. Rev. A* **61**, 052306 (2000).
161. Osborne, T. J. & Verstraete, F. General Monogamy Inequality for Bipartite Qubit Entanglement. *Phys. Rev. Lett.* **96**, 220503 (2006).
162. Ou, Y.-C. Violation of monogamy inequality for higher-dimensional objects. *Phys. Rev. A* **75**, 034305 (2007).
163. Streltsov, A., Adesso, G., Piani, M. & Bruß, D. Are General Quantum Correlations Monogamous? *Phys. Rev. Lett.* **109**, 050503 (2012).
164. Lancien, C. et al. Should Entanglement Measures be Monogamous or Faithful? *Phys. Rev. Lett.* **117**, 060501 (2016).
165. Christandl, M. & Winter, A. "squashed entanglement": An additive entanglement measure. *J. Math. Phys.* **45**, 829–840 (2004).
166. Osterloh, A. & Siewert, J. Constructing *n*-qubit entanglement monotones from antilinear operators. *Phys. Rev. A* **72**, 012337 (2005).
167. Gour, G. & Wallach, N. R. Classification of Multipartite Entanglement of All Finite Dimensionality. *Phys. Rev. Lett.* **111**, 060502 (2013).
168. Jungnitsch, B., Moroder, T. & Gühne, O. Taming Multiparticle Entanglement. *Phys. Rev. Lett.* **106**, 190502 (2011).
169. Huber, M. & Sengupta, R. Witnessing Genuine Multipartite Entanglement with Positive Maps. *Phys. Rev. Lett.* **113**, 100501 (2014).
170. Lancien, C., Gühne, O., Sengupta, R. & Huber, M. Relaxations of separability in multipartite systems: Semidefinite programs, witnesses and volumes. *J. Phys. A: Math. Theor.* **48**, 505302 (2015).
171. Clivaz, F., Huber, M., Lami, L. & Murta, G. Genuine-multipartite entanglement criteria based on positive maps. *J. Math. Phys.* **58**, 082201 (2017).
172. Bourennane, M. et al. Experimental Detection of Multipartite Entanglement using Witness Operators. *Phys. Rev. Lett.* **92**, 087902 (2004).
173. Hein, M. et al. in *Quantum Computers, Algorithms and Chaos*. Vol. 162 (eds Casati, G., Shepelyansky, D. L., Zoller, P. & Benenti, G.) 115–218 (IOS Press, 2005).
174. Bergmann, M. & Gühne, O. Entanglement criteria for Dicke states. *J. Phys. A: Math. Theor.* **46**, 385304 (2013).
175. Tóth, G. & Gühne, O. Entanglement and Permutational Symmetry. *Phys. Rev. Lett.* **102**, 170503 (2009).
176. Gühne, O. & Seevinck, M. Separability criteria for genuine multiparticle entanglement. *New J. Phys.* **12**, 053002 (2010).
177. Huber, M., Mintert, F., Gabriel, A. & Hiesmayr, B. C. Detection of High-Dimensional Genuine Multipartite Entanglement of Mixed States. *Phys. Rev. Lett.* **104**, 210501 (2010).
178. Tóth, G., Moroder, T. & Gühne, O. Evaluating Convex Roof Entanglement Measures. *Phys. Rev. Lett.* **114**, 160501 (2015).
179. Sperling, J. & Vogel, W. Multipartite Entanglement Witnesses. *Phys. Rev. Lett.* **111**, 110503 (2013).
180. Kitagawa, M. & Ueda, M. Squeezed spin states. *Phys. Rev. A* **47**, 5138–5143 (1993).
181. Wineland, D. J., Bollinger, J. J., Itano, W. M. & Heinzen, D. J. Squeezed atomic states and projection noise in spectroscopy. *Phys. Rev. A* **50**, 67–88 (1994).
182. Sørensen, A., Duan, L.-M., Cirac, J. I. & Zoller, P. Many-particle entanglement with Bose-Einstein condensates. *Nature* **409**, 63–66 (2001).
183. Tóth, G., Knapp, C., Gühne, O. & Briegel, H. J. Optimal Spin Squeezing Inequalities Detect Bound Entanglement in Spin Models. *Phys. Rev. Lett.* **99**, 250405 (2007).
184. Tóth, G., Knapp, C., Gühne, O. & Briegel, H. J. Spin squeezing and entanglement. *Phys. Rev. A* **79**, 042334 (2009).
185. Vitagliano, G., Hyllus, P., Egusquiza, I. L. & Tóth, G. Spin Squeezing Inequalities for Arbitrary Spin. *Phys. Rev. Lett.* **107**, 240502 (2011).
186. Vitagliano, G., Apellaniz, I., Egusquiza, I. L. & Tóth, G. Spin squeezing and entanglement for an arbitrary spin. *Phys. Rev. A* **89**, 032307 (2014).
187. Tura, J. et al. Detecting nonlocality in many-body quantum states. *Science* **344**, 1256–1258 (2014).
188. Lücke, B. et al. Detecting Multiparticle Entanglement of Dicke States. *Phys. Rev. Lett.* **112**, 155304 (2014).
189. He, Q. Y., Peng, S.-G., Drummond, P. D. & Reid, M. D. Planar quantum squeezing and atom interferometry. *Phys. Rev. A* **84**, 022107 (2011).
190. Pezzè, L. & Smerzi, A. Entanglement, Nonlinear Dynamics, and the Heisenberg Limit. *Phys. Rev. Lett.* **102**, 100401 (2009).
191. Hyllus, P. et al. Fisher information and multiparticle entanglement. *Phys. Rev. A* **85**, 022321 (2012).
192. Gessner, M., Pezzè, L. & Smerzi, A. Resolution-enhanced entanglement detection. *Phys. Rev. A* **95**, 032326 (2017).
193. Vollbrecht, K. G. H. & Cirac, J. I. Delocalized Entanglement of Atoms in Optical Lattices. *Phys. Rev. Lett.* **98**, 190502 (2007).
194. Cramer, M., Plenio, M. B. & Wunderlich, H. Measuring Entanglement in Condensed Matter Systems. *Phys. Rev. Lett.* **106**, 020401 (2011).
195. Dowling, M. R., Doherty, A. C. & Bartlett, S. D. Energy as an entanglement witness for quantum many-body systems. *Phys. Rev. A* **70**, 062113 (2004).
196. Tóth, G. Entanglement witnesses in spin models. *Phys. Rev. A* **71**, 010301 (2005).
197. Wieśniak, M., Vedral, V. & Brukner, Č. Magnetic susceptibility as a macroscopic entanglement witness. *New J. Phys.* **7**, 258 (2005).
198. Brukner, Č., Vedral, V. & Zeilinger, A. Crucial role of quantum entanglement in bulk properties of solids. *Phys. Rev. A* **73**, 012110 (2006).
199. Hauke, P., Heyl, M., Tagliacozzo, L. & Zoller, P. Measuring multipartite entanglement through dynamic susceptibilities. *Nat. Phys.* **12**, 778 (2016).
200. Cramer, M. et al. Spatial entanglement of bosons in optical lattices. *Nat. Commun.* **4**, 2161 (2013).
201. Marty, O. et al. Quantifying entanglement with scattering experiments. *Phys. Rev. B* **89**, 125117 (2014).
202. Fukuhara, T. et al. Spatially Resolved Detection of a Spin-Entanglement Wave in a Bose-Hubbard Chain. *Phys. Rev. Lett.* **115**, 035302 (2015).
203. Dai, H.-N. et al. Generation and detection of atomic spin entanglement in optical lattices. *Nat. Phys.* **12**, 783–787 (2016).
204. Islam, R. et al. Measuring entanglement entropy in a quantum many-body system. *Nature* **528**, 77 (2015).
205. Gross, D., Flammia, S. T. & Eisert, J. Most Quantum States Are Too Entangled To Be Useful As Computational Resources. *Phys. Rev. Lett.* **102**, 190501 (2009).
206. Terhal, B. M. Bell inequalities and the separability criterion. *Phys. Lett. A* **271**, 319–326 (2000).
207. Shalm, L. K. et al. Three-photon energy–time entanglement. *Nat. Phys.* **9**, 19–22 (2013).
208. Żukowski, M., Zeilinger, A. & Weinfurter, H. Entangling Photons Radiated by Independent Pulsed Sources. *Ann. NY Acad. Sci.* **755**, 91–102 (1995).
209. Pan, J.-W., Daniell, M., Gasparoni, S., Weihs, G. & Zeilinger, A. Experimental Demonstration of Four-Photon Entanglement and High-Fidelity Teleportation. *Phys. Rev. Lett.* **86**, 4435–4438 (2001).
210. Bouwmeester, D., Pan, J.-W., Daniell, M., Weinfurter, H. & Zeilinger, A. Observation of Three-Photon Greenberger-Horne-Zeilinger Entanglement. *Phys. Rev. Lett.* **82**, 1345–1349 (1999).
211. Pan, J.-W., Bouwmeester, D., Daniell, M., Weinfurter, H. & Zeilinger, A. Experimental test of quantum nonlocality in three-photon Greenberger-Horne-Zeilinger entanglement. *Nature* **403**, 515–519 (2000).
212. Wang, X.-L. et al. Experimental Ten-Photon Entanglement. *Phys. Rev. Lett.* **117**, 210502 (2016).
213. Graffitti, F., Barrow, P., Proietti, M., Kundys, D. & Fedrizzi, A. Independent high-purity photons created in domain-engineered crystals. *Optica* **5**, 514–517 (2018).
214. Malik, M. et al. Multi-photon entanglement in high dimensions. *Nat. Photon.* **10**, 248–252 (2016).
215. Leach, J., Padgett, M. J., Barnett, S. M., Franke-Arnold, S. & Courtial, J. Measuring the Orbital Angular Momentum of a Single Photon. *Phys. Rev. Lett.* **88**, 257901 (2002).
216. Erhard, M., Malik, M., Krenn, M. & Zeilinger, A. Experimental GHZ Entanglement beyond Qubits. *Nat. Photonics* **12**, 759–764 (2018).

217. Krenn, M., Malik, M., Fickler, R., Lapkiewicz, R. & Zeilinger, A. Automated Search for new Quantum Experiments. *Phys. Rev. Lett.* **116**, 090405 (2016).
218. Melnikov, A. A. et al. Active learning machine learns to create new quantum experiments. *Proc. Natl. Acad. Sci. U. S. A.* **115**, 1221–1226 (2018).
219. Friis, N. et al. Observation of Entangled States of a Fully Controlled 20-Qubit System. *Phys. Rev. X* **8**, 021012 (2018).
220. Leibfried, D. et al. Creation of a six-atom 'Schrödinger cat' state. *Nature* **438**, 639–642 (2005).
221. Häffner, H. et al. Scalable multiparticle entanglement of trapped ions. *Nature* **438**, 643–646 (2005).
222. Monz, T. et al. 14-Qubit Entanglement: Creation and Coherence. *Phys. Rev. Lett.* **106**, 130506 (2011).
223. Kaufmann, H. et al. Scalable Creation of Long-Lived Multipartite Entanglement. *Phys. Rev. Lett.* **119**, 150503 (2017).
224. Cramer, M. & Plenio, M. B. Reconstructing quantum states efficiently. Preprint at https://arxiv.org/abs/1002.3780 (2010).
225. Cramer, M. et al. Efficient quantum state tomography. *Nat. Commun.* **1**, 149 (2010).
226. Flammia, S. T., Gross, D., Bartlett, S. D. & Somma, R. Heralded Polynomial-Time Quantum State Tomography. Preprint at https://arxiv.org/abs/1002.3839 (2010).
227. Lanyon, B. P. et al. Efficient tomography of a quantum many-body system. *Nat. Phys.* **13**, 1158–1162 (2017).
228. Jurcevic, P. et al. Quasiparticle engineering and entanglement propagation in a quantum many-body system. *Nature* **511**, 202–205 (2014).
229. Hamley, C. D., Gerving, C. S., Hoang, T. M., Bookjans, E. M. & Chapman, M. S. Spin-nematic squeezed vacuum in a quantum gas. *Nat. Phys.* **8**, 305–308 (2012).
230. Kunkel, P. et al. Spatially distributed multipartite entanglement enables EPR steering of atomic clouds. *Science* **360**, 413–416 (2018).
231. Orzel, C., Tuchman, A. K., Fenselau, M. L., Yasuda, M. & Kasevich, M. A. Squeezed States in a Bose-Einstein Condensate. *Science* **291**, 2386–2389 (2001).
232. Esteve, J., Gross, C., Weller, A., Giovanazzi, S. & Oberthaler, M. K. Squeezing and entanglement in a Bose-Einstein condensate. *Nature* **455**, 1216–1219 (2008).
233. Riedel, M. F. et al. Atom-chip-based generation of entanglement for quantum metrology. *Nature* **464**, 1170–1173 (2010).
234. Gross, C., Zibold, T., Nicklas, E., Esteve, J. & Oberthaler, M. K. Nonlinear atom interferometer surpasses classical precision limit. *Nature* **464**, 1165–1169 (2010).
235. Ockeloen, C. F., Schmied, R., Riedel, M. F. & Treutlein, P. Quantum Metrology with a Scanning Probe Atom Interferometer. *Phys. Rev. Lett.* **111**, 143001 (2013).
236. Berrada, T. et al. Integrated Mach-Zehnder interferometer for Bose-Einstein condensates. *Nat. Commun.* **4**, 2077 (2013).
237. Muessel, W., Strobel, H., Linnemann, D., Hume, D. B. & Oberthaler, M. K. Scalable Spin Squeezing for Quantum-Enhanced Magnetometry with Bose-Einstein Condensates. *Phys. Rev. Lett.* **113**, 103004 (2014).
238. Kuzmich, A., Mandel, L. & Bigelow, N. P. Generation of Spin Squeezing via Continuous Quantum Nondemolition Measurement. *Phys. Rev. Lett.* **85**, 1594–1597 (2000).
239. Appel, J. et al. Mesoscopic atomic entanglement for precision measurements beyond the standard quantum limit. *Proc. Natl. Acad. Sci. U. S. A.* **106**, 10960–10965 (2009).
240. Sewell, R. J. et al. Ultrasensitive Atomic Spin Measurements with a Nonlinear Interferometer. *Phys. Rev. X* **4**, 021045 (2014).
241. Inoue, R., Tanaka, S.-I.-R., Namiki, R., Sagawa, T. & Takahashi, Y. Unconditional Quantum-Noise Suppression via Measurement-Based Quantum Feedback. *Phys. Rev. Lett.* **110**, 163602 (2013).
242. Chen, Z., Bohnet, J. G., Sankar, S. R., Dai, J. & Thompson, J. K. Conditional Spin Squeezing of a Large Ensemble via the Vacuum Rabi Splitting. *Phys. Rev. Lett.* **106**, 133601 (2011).
243. Zhang, H. et al. Collective State Measurement of Mesoscopic Ensembles with Single-Atom Resolution. *Phys. Rev. Lett.* **109**, 133603 (2012).
244. Bohnet, J. G. et al. Reduced spin measurement back-action for a phase sensitivity ten times beyond the standard quantum limit. *Nat. Photon* **8**, 731–736 (2014).
245. Hosten, O., Engelsen, N. J., Krishnakumar, R. & Kasevich, M. A. Measurement noise 100 times lower than the quantum-projection limit using entangled atoms. *Nature* **529**, 505–508 (2016).
246. Cox, K. C., Greve, G. P., Weiner, J. M. & Thompson, J. K. Deterministic Squeezed States with Collective Measurements and Feedback. *Phys. Rev. Lett.* **116**, 093602 (2016).
247. Fernholz, T. et al. Spin Squeezing of Atomic Ensembles via Nuclear-Electronic Spin Entanglement. *Phys. Rev. Lett.* **101**, 073601 (2008).
248. Hald, J., Sørensen, J. L., Schori, C. & Polzik, E. S. Spin Squeezed Atoms: A Macroscopic Entangled Ensemble Created by Light. *Phys. Rev. Lett.* **83**, 1319–1322 (1999).
249. Kuzmich, A., Mølmer, K. & Polzik, E. S. Spin Squeezing in an Ensemble of Atoms Illuminated with Squeezed Light. *Phys. Rev. Lett.* **79**, 4782–4785 (1997).
250. McConnell, R., Zhang, H., Hu, J., Ćuk, S. & Vuletić, V. Entanglement with negative wigner function of almost 3,000 atoms heralded by one photon. *Nature* **519**, 439–442 (2015).
251. Julsgaard, B., Kozhekin, A. & Polzik, E. S. Experimental long-lived entanglement of two macroscopic objects. *Nature* **413**, 400–403 (2001).
252. Behbood, N. et al. Generation of Macroscopic Singlet States in a Cold Atomic Ensemble. *Phys. Rev. Lett.* **113**, 093601 (2014).
253. Colangelo, G., Ciurana, F. M., Bianchet, L. C., Sewell, R. J. & Mitchell, M. W. Simultaneous tracking of spin angle and amplitude beyond classical limits. *Nature* **543**, 525–528 (2017).
254. Peise, J. et al. Satisfying the Einstein-Podolsky-Rosen criterion with massive particles. *Nat. Commun.* **6**, 8984 (2015).
255. Hoang, T. M. et al. Adiabatic quenches and characterization of amplitude excitations in a continuous quantum phase transition. *Proc. Natl. Acad. Sci. U. S. A.* **113**, 9475–9479 (2016).
256. Luo, X.-Y. et al. Deterministic entanglement generation from driving through quantum phase transitions. *Science* **355**, 620–623 (2017).
257. Engelsen, N. J., Krishnakumar, R., Hosten, O. & Kasevich, M. A. Bell Correlations in Spin-Squeezed States of 500 000 Atoms. *Phys. Rev. Lett.* **118**, 140401 (2017).
258. Fadel, M., Zibold, T., Décamps, B. & Treutlein, P. Spatial entanglement patterns and Einstein-Podolsky-Rosen steering in Bose-Einstein condensates. *Science* **360**, 409–413 (2018).
259. Wootters, W. K. & Fields, B. D. Optimal state-determination by mutually unbiased measurements. *Ann. Phys.* **191**, 363–381 (1989).
260. Asadian, A., Erker, P., Huber, M. & Klöckl, C. Heisenberg-Weyl Observables: Bloch vectors in phase space. *Phys. Rev. A* **94**, 010301 (2016).
261. Tóth, G. & Gühne, O. Detecting Genuine Multipartite Entanglement with Two Local Measurements. *Phys. Rev. Lett.* **94**, 060501 (2005).
262. Laskowski, W., Markiewicz, M., Paterek, T. & Żukowski, M. Correlation-tensor criteria for genuine multiqubit entanglement. *Phys. Rev. A* **84**, 062305 (2011).
263. Tiranov, A. et al. Temporal Multimode Storage of Entangled Photon Pairs. *Phys. Rev. Lett.* **117**, 240506 (2016).

Acknowledgements
The authors acknowledge support from the Austrian Science Fund (FWF) through the START project Y879-N27 and from the joint Czech–Austrian project MultiQUEST (I3053-N27 and GF17-33780L). N.F. acknowledges support from the FWF through project P 31339-N27. M.M. acknowledges support from the QuantERA ERA-NET co-fund (FWF Project I3773-N36) and from the UK Engineering and Physical Sciences Research Council (EPSRC) (EP/P024114/1). G.V. acknowledges support from the FWF through the Lise-Meitner project M 2462-N27.

Author contributions
All authors contributed to all aspects of manuscript preparation, revision, and editing.

Competing interests
The authors declare no competing interests.